



HAL
open science

Structural imaging of hippocampal subfields in healthy aging and Alzheimer's disease

Robin de Flores, Renaud La Joie, Gaël Chételat

► **To cite this version:**

Robin de Flores, Renaud La Joie, Gaël Chételat. Structural imaging of hippocampal subfields in healthy aging and Alzheimer's disease. *Neuroscience*, 2015, 309, pp.29-50. 10.1016/j.neuroscience.2015.08.033 . inserm-01668526

HAL Id: inserm-01668526

<https://inserm.hal.science/inserm-01668526v1>

Submitted on 20 Dec 2017

HAL is a multi-disciplinary open access archive for the deposit and dissemination of scientific research documents, whether they are published or not. The documents may come from teaching and research institutions in France or abroad, or from public or private research centers.

L'archive ouverte pluridisciplinaire **HAL**, est destinée au dépôt et à la diffusion de documents scientifiques de niveau recherche, publiés ou non, émanant des établissements d'enseignement et de recherche français ou étrangers, des laboratoires publics ou privés.

Structural imaging of hippocampal subfields in healthy aging and Alzheimer's disease

Robin de Flores^{1,2,3,4,*}, Renaud La Joie^{1,2,3,4,*#}, Gaël Chételat^{1,2,3,4}

1 INSERM U1077,

2 Université de Caen Basse-Normandie, UMR-S1077,

3 Ecole Pratique des Hautes Etudes, UMR-S1077,

4 CHU de Caen, U1077, Caen, France

* Authors contributed equally to this work

corresponding author, lajoie@cyceron.fr

Abstract

Hippocampal atrophy, as evidenced using magnetic resonance imaging (MRI), is one of the most validated, easily accessible and widely used biomarkers of Alzheimer's disease (AD). However, its imperfect sensitivity and specificity have highlighted the need to improve the analysis of MRI data. Based on neuropathological data showing a differential vulnerability of hippocampal subfields to AD processes, neuroimaging researchers have tried to capture corresponding morphological changes within the hippocampus.

The present review provides an overview of the methodological developments that allow the assessment of hippocampal subfield morphology *in vivo*, and summarizes the results of studies looking at the effects of AD and normal aging on these structures.

Most studies highlighted a focal atrophy of the CA1 subfield in the early (predementia or even preclinical) stages of AD, before atrophy becomes more widespread at the dementia stage, consistent with the pathological literature. Preliminary studies have indicated that looking at this focal atrophy pattern rather than standard whole hippocampus volumetry improves diagnostic accuracy at the Mild Cognitive Impairment (MCI) stage. However, controversies remain regarding changes in hippocampal subfield structure in normal aging and regarding correlations between specific subfield volume and memory abilities, very likely because of the strong methodological variability between studies.

Overall, hippocampal subfield analysis has proven to be a promising technique in the study of AD. However, harmonization of segmentation protocols and studies on larger samples are needed to enable accurate comparisons between studies and to confirm the clinical utility of these techniques.

Keywords

Hippocampus; magnetic resonance imaging; aging; Alzheimer's disease; CA1; biomarker

Highlights:

- Hippocampal subfield structure can be assessed *in vivo* with (high-resolution) MRI
- AD-related atrophy is initially focal (in CA1) before spreading to other subfields
- This pattern of atrophy could be a sensitive biomarker for early AD detection
- The effect of age and specific memory-volume correlations are less clear
- Variations in methods and segmentation protocols cause important discrepancies

1. Introduction

Although the term “hippocampus” was first used in 1587 by Arantius¹, it was only in the second part of the 20th century that scientists got the opportunity to thoroughly study this small medial temporal lobe structure, which has become one of the most scrutinized regions of the brain. Major advances were first made through the examination of patients with hippocampal lesions, the most famous being Henry Molaison (Scoville and Milner, 1957; see Squire, 2009 for review). More recently, the development of brain imaging has assisted researchers in investigating the role of the hippocampus in episodic memory processes in healthy individuals (Squire et al., 1992; Tulving and Markowitsch, 1998; see Spaniol et al., 2009 for review), as well as in patients with hippocampal damage, providing evidence that this structure is vulnerable to myriad neurological and psychiatric diseases (Geuze et al., 2005a; Small et al., 2011). Because of its important prevalence in the elderly and major socio-economic impact (Alzheimer’s Association, 2014; DiLuca and Olesen, 2014) Alzheimer’s disease (AD) is probably the most documented example of these conditions.

For more than two decades, the volume of the whole hippocampus has been assessed through manual delineation of the structure’s contours on anatomical images, classically T1-weighted isotropic magnetic resonance imaging (MRI) scans. This method has been used in the study of AD since the late 80’s (Seab et al., 1988), and has led to a tremendous number of publications in the field of neuroimaging. More recently, several automatic segmentation methods have been developed (eg. Brewer et al., 2009; Chupin et al., 2009; Fischl et al., 2002; Leung et al., 2010; Morra et al., 2008; Patenaude et al., 2011), enabling less time-consuming and more reproducible segmentations of the structure. From this perspective, major efforts

¹ who hesitated between the terms “sea horse” and “silkworm”, see Duvernoy (2005) and El-Falougy and Benuska (2006) for further details on the nomenclature and its evolution.

have been made to provide fully automated methods that could be used in clinical routine (Suppa et al., 2015a, 2015b).

While most of the imaging literature has studied the hippocampus as a single unitary entity, it is acknowledged that this structure is heterogeneous and can be divided into subregions with different functions, connectivity to other brain regions and vulnerability to disease (Aggleton, 2012; Maruszak and Thuret, 2014; Small et al., 2011). This heterogeneity is found both along the anterior-posterior axis of the hippocampus and across its different cytoarchitectonic subfields, which include the cornu ammonis fields (CA1–CA4²), the dentate gyrus (DG), and the subiculum. The idea of distinguishing hippocampal substructures from neuroimaging data is not new; a few authors have measured the volume of hippocampal regions along the anterior-posterior axis, namely the head, body and tail (see Poppenk et al., 2013 for a discussion on strategies for long-axis segmentation), and have explored differential effects of aging or disease across these substructures (Driscoll et al., 2003; Gordon et al., 2013; Jack et al., 1997; Malykhin et al., 2008; La Joie et al., 2013), or assessed anterior-posterior gradient in normal hippocampal function and connectivity (Aggleton, 2012; Poppenk et al., 2013; La Joie et al., 2014a; Chase et al., 2015; Adnan et al., 2015). However, it is only more recently, with the development of more sophisticated neuroimaging methods and the emergence of high field MR scanners providing high (i.e. submillimetric) resolution images, that the assessment of the hippocampal subfields has become accessible to human neuroimaging.

In the present review, we offer to give an overview of these methodological advances, summarize the results of structural imaging studies assessing the effects of AD and healthy

² However, there are still controversies regarding the existence of CA4 as a distinct entity ; according to some authors, these neurons probably belong to the hilar region of CA3 (for discussion see Schultz and Engelhardt 2014)

aging on hippocampal subfields, as well as the potential interest of these techniques, both in terms of diagnostic value and for the understanding of memory deficits.

2. From the hippocampus to hippocampal subfields: 15 years of technical and methodological progresses.

2.1. Indirect surface-based approaches using computational neuroanatomy tools

In the early 2000's, new approaches were developed to study the shape of the hippocampus and these methods gained popularity in assessing age or disease-related modifications in hippocampal morphology beyond volumetric changes. These various techniques (eg. *large deformation high-dimensional brain mapping* (Csernansky et al., 2000; Wang et al., 2003), *radial atrophy* (Apostolova et al., 2006a; Frisoni et al., 2006; Thompson et al., 2004) or *spherical harmonics* (Gerardin et al., 2009; Lindberg et al., 2012; Sarazin et al., 2010)), are generally based on four main steps: 1) (manual or automated) segmentation of the whole hippocampus, 2) surface reconstruction, i.e. converting segmentations to surface meshes, 3) across subject alignment of the surfaces, 4) between subject comparison of hippocampal surfaces, usually through the computation of displacement vectors indicating the difference between each subject and a reference (either an average surface or a template). Eventually, these methods provide images showing local areas of inward or outward displacement of the surface in relation to age, disease, or cognitive performance. From these measures, volumetric changes in subfields are inferred, depending on the location of these modifications on the hippocampal surface and using a 3-dimensional atlas of hippocampal subfields (for examples, see Figure 1). It should be acknowledged that these sophisticated methods only provide indirect indication of subfield atrophy, and it is not clear how the atrophy of the deepest regions of the hippocampus (ie CA4-DG) would impact the outer surface of the structure.

Our lab developed a variant of these methods; instead of analyzing surfaces directly, we used the Voxel Based Morphometry (VBM) procedure (Ashburner and Friston, 2000; Ashburner, 2007) to analyze grey matter volume changes in every voxel of the brain, and projected the subsequent results onto a 3D hippocampal surface (Chételat et al., 2008; Fouquet et al., 2012; La Joie et al., 2010). Other groups (Atienza et al., 2011; Thomann et al., 2013; Ziegler et al., 2011) also used VBM to assess the volume of hippocampal subfields, extracting the volumes of regions of interests derived from probabilistic cytoarchitectonic atlases (Amunts et al., 2005).

2.2. Subfield volumetry

2.2.1. Volumetry from high-resolution images: multiple segmentation protocols applied on various images.

2.2.1.1. Manual delineation

Over the past years, with the introduction of higher fields MRI scanners (3T, 4T, 7T or 9.4T), several high-resolution sequences centered on the medial temporal lobe have been developed, for both structural and functional MRI studies. These oblique coronal images, oriented perpendicular to the longitudinal axis of the hippocampus, have enough contrast and in-plane resolution (i.e. submillimetric) to visualize internal details within the hippocampus, therefore providing anatomic landmarks that can be used to distinguish subregions and perform direct volumetric studies. However, it is important to keep in mind that, in spite of this high resolution, it is still not yet possible to directly visualize the border between two contiguous subfields (eg. CA1 and subiculum): high-resolution neuroimaging is not *in vivo* histology. Subfield boundaries therefore rely on landmarks derived from anatomical atlases and geometric rules that are set to reach a compromise between reliability/reproducibility and

validity: *in vivo* volumetric measurements are only approximations of the actual subfield volumes.

The strong between-study heterogeneity of segmentation protocols should also be highlighted, as multiple differences can be found in terms of i) number of segmented subfields, ii) which subfields are segmented separately or grouped together, iii) subfield borders and, iv) whether subfield segmentation is performed on the full length of the hippocampus or only on the body (see figure 2 for an illustration of this heterogeneity). This variability is not only due to differences in the atlases used as references, but also to the technical characteristics of the MRI data: scanner field strength (usually between 3T and 7T), image weighting (usually T2, but also proton density) and resolution (see the Tables for a global overview of the sequence variability). For example, Wisse et al. (2012) acquired T2-weighted images with isotropic voxels (0.7 x 0.7 x 0.7 mm) on a 7T scanner to segment 5 regions (subiculum, CA1, CA2, CA3, CA4-DG) along the full axis of the hippocampus, while we manually delineate 3 regions (subiculum, CA1, CA2-3-4-DG) along the entire hippocampus using proton density weighted images acquired on a 3T scanner with a resolution of 0.375 x 0.375 x 2 mm (de Flores et al., 2015; La Joie et al., 2013, 2010), and Mueller et al. (2007, 2009, 2010) use T2-weighted images with a 0.4 x 0.4 x 2 mm resolution from a 4T scanner to delineate 4 regions (subiculum, CA1, CA2, CA3-DG) in the hippocampal body. For a deeper and more exhaustive analysis of the various elements of between-study variability - which is not the purpose of the current review – the reader is referred to a very recent report from a group of hippocampal subfield experts who qualitatively and quantitatively compared 21 segmentation protocols (Yushkevich et al., 2015a).

In addition to volumetric analyses of hippocampal subfields, alternative methods have been proposed to analyze these medial temporal lobe-centered high-resolution images. Notably,

some authors have used a cortical unfolding technique to enhance the visibility of the convoluted medial temporal lobe cortex by flattening the entire gray matter volume into two-dimensional space (Burggren et al., 2008; Donix et al., 2010a, 2010b; Ekstrom et al., 2009). This allows the thickness of the cortical ribbon throughout each identified subregion to be examined separately, and could provide sensitive information that could be complementary, and not redundant with volumetric measures.

Kerchner et al. (2010, 2012, 2013, 2014) developed another approach that was directly influenced by several neuropathological studies showing that AD-related neurodegeneration is not only subfield-, but also strata-specific, with a stronger vulnerability of the synapse-rich apical neuropil layer (the stratum radiatum and stratum lacunosum-moleculare, SRLM) as compared to the cell body layer (the stratum pyramidale, SP). Using 7T T2-weighted MR images with ultra high resolution (0.22 x 0.22 x 1.5 mm voxels), they measured different metrics in the body of the hippocampus, including the width (or thickness) of CA1-SRLM, defined as the hypointense band between the more intense DG and CA1-SP cell layers.

2.2.1.2. Toward automated methods

Similar to global hippocampal volumetry (see Dill et al., 2014 for a review), a few automatic methods have been developed to facilitate subfield assessment in research and for potential clinical application without requiring as much time, labor and anatomical expertise as manual delineation.

Notably, a group from the University of Pennsylvania initially developed an open-source, semi-automatic method called Automatic Segmentation of Hippocampal Subfields (ASHS), designed to be used on high-resolution anisotropic T2 images (Yushkevich et al., 2010). This algorithm initially relied on the segmentation protocol developed by Mueller et al. (2007), so that it was restricted to the hippocampal body, and was used in the context of aging and AD

(Pluta et al., 2012). ASHS was recently improved (Yushkevich et al., 2015b) to i) identify more numerous hippocampal subfields and parahippocampal subregions, ii) segment these along the full length of the hippocampus, iii) allow both volume and thickness analysis. This updated, fully automated version of ASHS requires a classical T1-weighted image in addition to the high-resolution T2-weighted MRI.

2.2.2. Subfield volumetry using standard 1mm³ isotropic T1-weighted images

In parallel, methods to measure the volume of hippocampal subfields using standard ($\approx 1\text{mm}^3$ isotropic) images have also been developed. The most widely used is that implemented in FreeSurfer 5.3, and has been developed and validated using ultra-high resolution *in vivo* T1-weighted images (Van Leemput et al., 2009). Using this technique, 10 region labels (including subfields *per se*, but also hippocampal fissure, choroid plexus, fimbria and inferior lateral ventricle) are propagated from an ultra-high resolution template by applying heuristic rules based on the anatomy of the whole hippocampus rather than using internal landmarks within the hippocampus (which are not visible on standard scans). Because this method is user-friendly and directly applicable to standard 1.5T or 3T T1-weighted scans, it has been used extensively over the last several years to study hippocampal changes related to development, aging and various conditions (Aas et al., 2014; Durazzo et al., 2013; Engvig et al., 2012; Ezzati et al., 2014; Francis et al., 2013; Hanseeuw et al., 2011; Haukvik et al., 2014; Hsu et al., 2014; Khan et al., 2014; Krogsrud et al., 2014; Kühn et al., 2014; Lim et al., 2012a, 2012b; Pereira et al., 2014, 2013; Tamnes et al., 2014; Teicher et al., 2012 among others).

However, some authors have recently expressed their concerns about the subfield segmentation tool implemented in FreeSurfer 5.3 (de Flores et al., 2015; Pluta et al., 2012; Wisse et al., 2014a; Yushkevich et al., 2015b), arguing that this method has not been

validated on the standard images on which it is commonly used. More precisely, doubts are cast upon the ability to distinguish (numerous) subfields using low-resolution images, but also about the boundaries of the parcellation scheme, which strongly differs from the majority of *in vivo* and imaging atlases. For instance, FreeSurfer 5.3's CA1 is the smallest subfield while CA2-3 is the biggest, which contrasts with histologic data showing the opposite (for discussion, see de Flores et al., 2015 and Wisse et al., 2014a, Yuschkevich et al., 2015). These specificities of the FreeSurfer 5.3 subfield segmentation package must be recognized when interpreting the abundance of results based on this broadly used but controversial method (see below).

Very recently, the creators of FreeSurfer 5.3 subfield segmentation tool have acknowledged the flaws of their initial method, notably explaining that “*The delineation protocol of the in vivo atlas was designed for the hippocampal body and did not translate well to the hippocampal head or tail*” (see the official website <https://surfer.nmr.mgh.harvard.edu/fswiki/HippocampalSubfieldSegmentation> ; note that the tool is now declared “deprecated”). Instead, they have developed an alternative tool implemented in FreeSurfer 6.0 (Iglesias et al., 2015). Briefly, this new method uses a specifically developed atlas developed from 15 subjects with *ex vivo* 7T MRI scans and comprised 13 different labels. Importantly, FreeSurfer 6.0 tool can be used using classical (isotropic) T1-weighted scans, specific (anisotropic) T2-weighted images, or both. As a consequence of these major changes, results are likely to be very different from those obtained with FreeSurfer 5.3. Indeed, Iglesias et al (2015) used both FreeSurfer 5.3 and 6.0 on T1-MRI from AD patients and normal controls and found important discrepancies, e.g. CA1 went from one of the least different to one of the most different subfields (see Iglesias et al 2015, table 6 and present review, Table 1). Results obtained with the FreeSurfer 6.0 thus appear more

accurate than its predecessor (see below); yet, because of its novelty, it has not been widely used and tested yet.

Another approach has been developed through the MAGeT-Brain (Multiple Automatically Generated Templates) algorithm, which minimises the number of input atlases needed (Pipitone et al., 2014) by creating a template library from a sample of the subject images. So far, MAGeT-Brain has been used on normal controls (Pipitone et al., 2014) and depressed patients (Treadway et al., 2015) to segment subfields on T1-weighted images using the 5 ultra-high resolution subfield images from the Winterburn atlas (Winterburn et al., 2013, healthy controls, age range = 29-57) as inputs. To date, this technique has not been used in aging or dementia, and future studies are needed to assess how the algorithm will handle the segmentation in elder individuals with major atrophy, and whether other (or additional) age-matched manually segmented subfield images are needed as inputs.

3. Alzheimer's disease

AD is the most common type of dementia, accounting for 60-80% of cases (Alzheimer's Association, 2014). Recent epidemiological studies estimated that 44.35 million people are affected by dementia worldwide and projected that the prevalence would reach 75.62 million by 2030 (Alzheimer's Disease International, 2013), mainly because of population aging. Although dementia is not the most prevalent brain disorder in Europe and other western countries, its global socio-economic impact is tremendous because of the high individual cost it causes (DiLuca and Olesen, 2014).

Pathologically, AD is characterized by two main pathological hallmarks: extracellular amyloid deposits composed of insoluble amyloid beta ($A\beta$) protein, and intra-neuronal neurofibrillary tangles (NFTs) containing hyperphosphorylated tau protein (Hyman et al., 2012; Khachaturian, 1985; Markesbery, 1997; Mirra et al., 1991; Montine et al., 2012). Along

with these two proteinopathies, AD is characterized by significant loss of neurons and synapses, resulting in brain shrinkage (see Duyckaerts et al., 2009 for review).

From a clinical perspective, AD is classically diagnosed at the dementia stage when cognitive deficits already significantly impact activities of daily living (McKhann et al., 1984). However, because of the progressive nature of cognitive decline and underlying pathology, it is now fully accepted that the disease is characterized by an asymptomatic or ‘preclinical’ stage (where pathological features are developing in individuals with normal cognition, as observed either at autopsy or *in vivo* using biomarkers), followed by a pre-dementia or prodromal stage, where symptoms are detectable but not sufficient to meet criteria for dementia. This later stage usually but not always corresponds to the clinically defined amnesic subtype of mild cognitive impairment (MCI), characterized by the presence of memory complaint together with isolated memory impairment as objectivized by a neuropsychological examination. However, (amnesic) MCI is a heterogeneous entity that can be due to various underlying neurological or psychiatric etiologies (Hughes et al., 2011). In a meta-analysis of 41 clinical studies of MCI patients with a minimal longitudinal follow up of 3 years, annual conversion rate to AD was estimated around 7% for MCI and almost 12% for amnesic MCI, while relative risk of AD (as compared to cognitively normal individuals) was around 9-fold (Mitchell and Shiri-Feshki, 2009). Yet, not all (amnesic) MCI patients develop AD or dementia, even after a decade, and a significant proportion of them remain stable or even revert to normal cognition during the follow up period (Ganguli et al., 2011; Koepsell and Monsell, 2012). This important variability in MCI outcomes stresses the need to develop methods and tools enabling the identification of the MCI patients who are the most likely to eventually progress to dementia, for both patients’ care and potential inclusion in clinical trials.

3.1. Hippocampal damage in AD: previous knowledge from neuropathology and global volumetry

The hippocampus is one of the major targets of AD pathological hallmarks, especially of neurofibrillary tangles (NFT) and neuron and neurite loss. In the hippocampus, NFT first target CA1, then the subiculum, CA2, CA3 and CA4/DG (Braak and Braak, 1991; Braak et al., 1993; Fukutani et al., 2000; Lace et al., 2009; Schönheit et al., 2004). As for neuronal loss, a histological study reported major losses in AD patients in CA1 (68%) as well as in the subiculum (47%) and hilus (25%) in comparison with age-matched controls (West et al., 1994). By contrast, no significant neuronal loss was found in cognitively normal elders with substantial neuritic A β plaques in their brain (West et al., 2004; Price et al., 2001). Moreover, Price et al. (2001) showed an incremental decrease in CA1 neurons from 29% in very mild AD patients to 38% in AD patients with severe dementia. Overall, neuronal loss has been found to predominate in the CA1 subfield in most studies (Kril et al., 2002; Padurariu et al., 2012; von Gunten et al., 2006), although discrepant findings have also been reported (Simic et al., 1997). Moreover, CA1 neuronal loss was found to correlate with the density of NFT (Fukutani et al., 2000; von Gunten et al., 2006).

In line with the pathological literature, neuroimaging studies have shown that the hippocampus is already significantly damaged at the time of AD (dementia) diagnosis: according to a meta-analysis of structural imaging studies including 700 patients with mild to moderate dementia, the volume loss is around 23-24% as compared to age-matched controls (Shi et al., 2009). Longitudinal studies conducted on cohorts of cognitively normal elders have reported that hippocampal atrophy is already present in the preclinical stage, ie before the stage of MCI (Bernard et al., 2014; Smith et al., 2012, 2007), up to 10 years before the diagnosis of dementia (Tondelli et al., 2012).

3.2.Subfield imaging in AD

3.2.1. Dementia and predementia stages

Table 1 summarizes the main results from studies conducted in patients with AD or MCI.

When comparing AD patients to healthy controls using surface-based techniques, studies have systematically described major inward surface deformation along the lateral zone of the hippocampus, which corresponds to the CA1 subfield (see Figure 1 for examples of subfield display on the surface). This result is consensual as it is independent from the specific method used: it has been reported using radial atrophy (Frisoni et al., 2008, 2006; Scher et al., 2007), large deformation high-dimensional brain mapping (Csernansky et al., 2000; Tang et al., 2014; Tepest et al., 2008; Wang et al., 2006, 2003), spherical harmonics (Gerardin et al., 2009; Lindberg et al., 2012) or a VBM-based analysis (Chételat et al., 2008); see Figure 1 for an illustration. In some studies, abnormalities were also found in medial regions of the surface, mostly corresponding to the (pre)subiculum (Frisoni et al., 2008, 2006; Wang et al., 2006) or even in all subfields (Apostolova et al., 2012; Chow et al., 2012, 2015). Using direct volumetry in AD patients, several studies reported significant atrophy in all, or almost all, investigated subfields (Adachi et al., 2003; Boutet et al., 2014; de Flores et al., 2015; Khan et al., 2014; La Joie et al., 2013; Li et al., 2013), the major atrophy being generally located in CA1 (La Joie et al., 2013; de Flores et al., 2015; Mueller et al., 2010). In a few studies, some subfields were (relatively) spared, namely CA3/DG (Mueller and Weiner, 2009; Mueller et al., 2010) or CA2 (Wisse et al., 2014b).

Among MCI patients, shape analysis identified a more focal pattern of atrophy, usually restricted to the lateral side of the hippocampus corresponding to CA1, and sometimes also including the subiculum (Chételat et al., 2008; Gerardin et al., 2009; Tang et al., 2014; Tepest et al., 2008). Volumetric studies showed a volume reduction predominant in CA1, and also

involving either CA3/DG (Yassa et al., 2010b), CA4/DG (Pluta et al., 2012) or the subiculum (de Flores et al., 2015; La Joie et al., 2013). In those two latter studies (performed in an overlapping sample), the mean volume loss in MCI patients was estimated at 20% for CA1 and 15% for the subiculum. Note that Mueller et al. specifically assessed the CA1-2 transition area and reported predominant atrophy in this region in MCI patients (Mueller and Weiner, 2009; Mueller et al., 2010). Negative findings (i.e. no significant atrophy in any hippocampal subfield) have also been reported, potentially because of low statistical power (Kerchner et al., 2013; Wisse et al., 2014b).

Interestingly, the relatively specific pattern found in MCI (CA1 alone or CA1 and subiculum) was even more pronounced in the patients that later converted to dementia (Apostolova et al., 2006b; Chételat et al., 2008), while transition from MCI to dementia seems to be associated with a spreading of atrophy to the rest of the hippocampus (Apostolova et al., 2010c; La Joie et al., 2013; Mueller et al., 2010).

A couple of studies (La Joie et al., 2013; Ye et al., 2014) have compared the pattern of hippocampal atrophy in MCI patients with and without A β pathology (A β ⁺ and A β ⁻, respectively), the former group being at higher risk of rapid cognitive decline (Doraiswamy et al., 2014) and the latter being considered less likely to be on the AD track (Albert et al., 2011). Both studies showed that A β ⁺ and A β ⁻ MCI showed significant atrophy of the CA1 subfield. The effect appeared stronger in the A β ⁺ patients but the difference between both patient groups was not significant and might simply reflect a difference in the sample size and associated statistical power (due to a higher number of A β ⁺ than A β ⁻ patients). Although these studies should be interpreted as preliminary because of their small sample sizes, they found similar results despite different methods: shape analysis (Ye et al., 2014) and manual volumetry on high-resolution images (La Joie et al., 2013). Pending replication in future

studies, this suggests that the preferential pattern of subfield atrophy observed in AD is independent from A β pathology.

Studies have also shown that CA1 and subiculum atrophy was present at a very early stage of AD, as it was detectable in cognitively healthy individuals that later developed MCI or AD (Apostolova et al., 2010b; Csernansky et al., 2005). Together with studies mentioned above showing an association between CA1 (and subiculum) atrophy and subsequent conversion from MCI to dementia, these reports stress the importance of hippocampal subfield measurements as sensitive markers of AD processes and emphasize their potential role as biomarkers for early AD detection.

It should be noted that studies using the FreeSurfer 5.3 automatic method reported discrepant findings as compared to the studies mentioned above that used different techniques. Thus, all FreeSurfer 5.3 studies have detected volume loss in the subiculum and the CA2/3 region in MCI and AD patients, while only a few articles (Khan et al., 2014; Li et al., 2013) also reported CA1 atrophy (See Table 1, bottom section). As mentioned above, this might be due to difference in subfield definition and boundaries used in FreeSurfer 5.3. More specifically, FreeSurfer 5.3's CA1 is smaller than in other protocols, and most of FreeSurfer 5.3's subiculum overlaps with what other protocols consider as CA1 (see de Flores et al., 2015 and Wisse et al., 2014a for further discussion). On the contrary, the new method implemented in FreeSurfer 6.0 seem to produce more coherent results, CA1 being one of the most strongly different subregions when considering MCI or AD patients compared to controls (Iglesias et al., 2015).

3.2.2. Cognitively intact individuals at risk for AD

To date, only a few studies have assessed hippocampal shape or subfield volumes in cognitively intact individuals at risk for AD, including carriers of the $\epsilon 4$ allele of the

Apolipoprotein E, healthy controls with amyloid β deposition, and individuals with isolated subjective memory complaint.

The $\epsilon 4$ allele of the apolipoprotein E (APOE4) is the largest genetic risk factor for sporadic AD (Corder et al., 1993; Farrer et al., 1997; Genin et al., 2011), and its detrimental effect (as compared to the more frequent $\epsilon 3$ allele) is dose-dependent: odds ratio for AD are 3.2 for $\epsilon 4/\epsilon 3$ carriers, and 14.9 for $\epsilon 4/\epsilon 4$ carriers (Farrer et al., 1997). Many studies have assessed the effect of APOE polymorphism on grey matter volume but only a few have examined the effects on hippocampal subfields. Overall, the findings converge to a detrimental effect on the cortical thickness or volume of the hippocampus in elderly and patients, although results diverged with regard to the affected subfield (see Table 2). A first group showed that cortical thickness was found to be lower in elderly APOE4 carriers compared with non-carriers in the subiculum (Burggren et al., 2008). In a subsequent study from the same group, Donix et al. (2010b) found that family history of AD and APOE4 status were independently associated with a thinner subiculum, with an additive effect of these two AD risk factors. In a longitudinal study of subfield thickness over two years, the same authors showed a stronger rate of atrophy in the subiculum (Donix et al., 2010b). By contrast, Kerchner et al. (2014) found a selective, dose dependent effect on the CA1-SRLM width (yet, controls were pooled with MCI and demented patients in this analysis), while Mueller et al. reported a detrimental effect of the $\epsilon 4$ allele on CA3/DG volume in healthy elderly, but not in middle aged individuals (Mueller and Weiner, 2009; Mueller et al., 2008). Overall, the important variability in these results makes it difficult to get a clear picture of the preferential effect of APOE4 on hippocampal subfield volume in asymptomatic individuals. The same discrepancy is found amongst studies assessing cortical atrophy at large (see Fouquet et al., 2014 for review).

Hippocampal subfield atrophy has also been assessed in another group of asymptomatic elderly at-risk for AD, namely, cognitively normal individuals with detectable A β pathology evidenced with either PET imaging or cerebro-spinal fluid measurements. Although these individuals are often considered as being in the first stage of the disease (Sperling et al., 2011), others prefer to refer to them as “asymptomatic at risk for AD” (Dubois et al., 2014, 2010) as it is still unsure whether A β pathology alone is sufficient to later develop clinical AD. The presence of A β was associated with significantly smaller hippocampal tail, presubiculum and subiculum volumes estimated with FreeSurfer 5.3 (Hsu et al., 2014). Using radial atrophy measurements and cerebro-spinal fluid measures, Apostolova et al. (2010a) did not identify any specific pattern of shape deformation associated with A β pathology. Using another type of shape analysis, Carmichael et al. (2012) showed that, in healthy elders, A β was related to subtle hippocampal shape patterns, mainly inward deformations in the inferior-anterior head as well as the superior and inferior body; however, these morphological changes were not interpreted in terms of subfield atrophy.

Lastly, to date, only one study has assessed patients with subjective memory complaint, known to be at-risk of later developing AD although they perform in the normal range on neuropsychological tests (Jessen et al., 2014). In their article, Tepest et al. (2008) reported a slight inward deformation restricted to CA1 as compared to non-complaining healthy controls. This pattern was qualitatively similar to AD and MCI patients but did not reach the level of significance.

3.3. Clinical interest of hippocampal subfield volumetry?

3.3.1. MRI as a positive diagnostic tool for AD.

According to the 30 year-old NINCDS-ADRDA criteria for AD that are still currently used in most clinical settings, imaging could be used to exclude potential organic causes of

symptoms, such as subdural hematoma, brain tumor, hydrocephalus and dementia associated with vascular disease (McKhann et al., 1984). However, at the time these criteria were developed, the neuroimaging literature was still limited and authors foresaw that “information should soon be available about the usefulness of MRI in the diagnosis of Alzheimer’s disease”. Indeed, after more than 2 decades of intense research, it has been proposed to use (MR and PET) imaging to highlight the presence of specific abnormalities, indicating a neurodegenerative process consistent with AD (Albert et al., 2011; Dubois et al., 2010, 2007; McKhann et al., 2011; Sperling et al., 2011), although experts are still debating about it (Dubois et al., 2014).

In this context, hippocampal volumetry appears as a natural candidate, and has therefore already been used in many research studies as a biomarker indicating AD-related degeneration at different stages of disease progression (eg. Jack et al., 2012; Knopman et al., 2012; Wirth et al., 2013). Recently, several experts have joined forces to establish a standard protocol for hippocampal segmentation (Boccardi et al., 2014, 2013a, 2013b, 2011; Bocchetta et al., 2014; Frisoni et al., 2014), in order to solve the major issue of high variability in hippocampus boundary definition and delineation procedure that limited inter-study comparability from previous works (Boccardi et al., 2011; Geuze et al., 2005b; Konrad et al., 2009). However, whole hippocampal volumetry is likely imperfect because of its rather low sensitivity and specificity (Frisoni et al., 2010), fueling the need for more accurate disease biomarkers, including subfield volumetry.

3.3.2. Subfields versus whole hippocampus: Improving AD detection?

To date, only a few studies have assessed the diagnostic value of high-resolution subfield volumetry and compared it to the classical whole hippocampus volumetry, but their results are highly consistent.

The first report by Mueller et al. (2010), showed that the CA1-2 transition area was superior to total hippocampal volume for distinction between 53 healthy controls and 20 patients with MCI: the area under the receiver operating characteristic curve (AUROC) was 0.83 for CA1/2 versus 0.72 for the entire hippocampus. Interestingly no subfield showed a significantly higher power than the whole hippocampus to discriminate the controls from 18 AD patients (AUROC= 0.81 for CA1/2 versus 0.75 for whole hippocampus, non-significant difference), suggesting that the superior discriminant capacity of hippocampal subfield volumetry over the whole hippocampus is limited to the prodementia stage. Using a semi-automated method, Pluta et al. (2012), showed that the left CA1 volume better discriminated 17 amnesic MCI patients from 28 controls than the total hippocampus (AUROC = 0.84 versus 0.76, $p=0.03$). The same conclusion was also reached in an independent study with a fully manual delineation technique showing that CA1 was more informative than the total hippocampus to distinguish 17 amnesic MCI patients from 40 elderly controls (AUROC = 0.88 versus 0.76, $p=0.05$; La Joie et al., 2013). In this study and similar to Mueller et al (2010), the superiority of subfield volumetry over total hippocampal measurement was not found when comparing AD patients to controls (AUROC = 0.92 for CA1 versus 0.91 for total hippocampus, non significant).

Altogether, these studies point to the increased sensitivity of subfield volumetry, and especially the CA1 or CA1/2 area, to detect morphological changes at the prodromal stage of MCI, but not at the dementia stage. This is consistent with the notion that NFT pathology, synaptic, neuronal and volumetric losses are focal in the first pathophysiological stages and progressively extend to the whole hippocampus to become global in the advanced stage of dementia (see section 3.2.1 above).

3.3.3. Subfield volumetry in a clinical setting?

It should be noted that these encouraging results emanate from monocentric studies mostly based on small groups of individuals and should therefore be considered with caution. This issue is to be addressed through the recent addition of a high-resolution hippocampal-centric T2 acquisition in a third of the sites that participate in the Alzheimer's Disease Neuroimaging Initiative (ADNI), a large multicentric longitudinal study of AD (Mueller et al., 2005).

In addition, these academic studies are based on highly selected individuals: both healthy controls and patients are usually free of major comorbidities and have limited history of psychiatric or cardiovascular disorders. This misrepresentation of the general population could constitute a bias in the assessment of diagnostic utility of hippocampal subfield volumetry, as recent reports have suggested that factors/conditions such as smoking (Durazzo et al., 2013), hypertension (Shing et al., 2011), multiple sclerosis (Sicotte et al., 2008), borderline personality disorder (Rossi et al., 2012) or depression (Huang et al., 2013; Wisse et al., 2015a) could have an impact on subfield volume, and notably on the subfields known to me the most sensitive to AD (CA1, CA1-2 areas). The higher prevalence of such factors in the general population as compared to these highly selected academic studies would probably increase the variability of subfield volumes and could lower the diagnostic interest of subfield imaging.

Similarly, the diagnostic value of subfield volumetry has only been assessed by comparing MCI or AD patients to healthy controls, without including other groups of non-AD demented patients. Therefore, the context of these studies strongly differ from clinical settings where differential diagnosis can be challenging - memory impairment / dementia can be due to various potential etiologies (Arlt, 2013) - and for which biomarkers could be very helpful. Indeed, it is well known that total hippocampal atrophy is found in multiple conditions (Fotuhi et al., 2012; Geuze et al., 2005a), which makes it poorly specific to AD

pathophysiological processes. Unfortunately, there is no current data supporting the idea that subfield volumetry would be more specific to AD than total hippocampal volumetry. Indeed, neuroimaging studies in other disorders are sparse and seem to indicate that CA1 (+/- subiculum) is also the subfield of strongest atrophy in dementia with Lewy body (Chow et al., 2012; Sabattoli et al., 2008), and various subtypes of frontotemporal lobar degeneration (La Joie et al., 2013; Lindberg et al., 2012). Similarly, neuropathological studies have reported a strong CA1 neuronal loss in patients with vascular dementia (Gemmell et al., 2012; Kril et al., 2002).

From a more practical point of view, the clinical feasibility of high-resolution hippocampus-centric MRI acquisitions is still uncertain because these scans are particularly prone to motion artifacts (for discussion, see La Joie et al., 2013; Mueller and Weiner, 2009). Lastly, the clinical use of such data would only be conceivable with automated and validated subfield segmentation tools that would not require the expertise and time of manual delineation.

To summarize, current data is limited but suggests that subfield volumetry improves the ability to detect AD-related changes, especially in early (predementia) stages of the disease. However, additional studies conducted in larger and more representative populations are needed to confirm the feasibility and the added value of the technique in a clinical setting.

4. Healthy aging

Several studies on brain structure, including but not restricted to the hippocampus, have compared the effects of AD, as an example of pathological aging, to the effects of “normal”, “healthy”, or “successful” aging, generally defined as the age-related changes that occur in the absence of significant cognitive disorder, i.e. disease-free aging. This is usually assessed by comparing the brain structure of young versus old cognitively intact individuals, assessing the

correlation between brain volume and age within a group of cognitively healthy individuals, or in longitudinal studies of individuals who remain free of cognitive deficit over a few years. Several neuroimaging studies have indicated that the human brain shrinks with age, and that brain shrinkage is selective and differential, not uniform or randomly distributed (Raz and Rodrigue, 2006; Sowell et al., 2003). Evidence also suggests that these structural changes explain some part of age-related changes in cognition (see Fjell and Walhovd, 2010; Lockhart and DeCarli, 2014 for recent reviews of the field).

However, the frontier between “normal” and “pathological” aging is not clear-cut as it is challenging to distinguish age-related changes from the effects of preclinical diseases, especially as the main risk factor for AD is advancing age (see Fjell et al., 2014a for a critical review on these concepts).

4.1. Studying aging: methodological considerations

Differences in reported results are frequent as cohorts and methods used to study aging greatly vary among studies. The most optimal way to assess genuine age-related changes is to perform longitudinal studies in which the effect of age is examined within subjects over time (Dotson et al., 2009; Driscoll et al., 2009; Fjell et al., 2009; Marcus et al., 2010; Raz et al., 2005, 2004; Resnick et al., 2003; Scahill et al., 2003; Thambisetty et al., 2010). Unfortunately, such studies are rare - because of their cost and attrition bias - and not yet capable of addressing age-related brain differences over several decades. As a consequence, cross sectional studies are more often conducted in order to estimate age-related changes, although they might produce inconsistent results when compared to longitudinal analyses (Pfefferbaum and Sullivan 2015). Indeed, the cross-sectional approach is easier to implement, but it suffers from major flaws including potential cohort bias and the influence of elder

individuals at the presymptomatic stage of a neurodegenerative disorder which may cause an overestimation of the age effect (Burgmans et al., 2009).

The considered age range is also a source of heterogeneity between studies (Walhovd et al., 2011) as some studies evaluate the effect of age over the entire adult lifespan (Mueller et al., 2007, 2009 ; Chételat et al., 2008 ; La Joie et al., 2010 ; Ziegler et al., 2010 ; Raz et al., 2014 ; de Flores et al., 2015 ; Pereira et al., 2014), while others only included elderly people (Wang et al., 2003, 2006 ; Frisoni et al., 2008 ; Apostolova et al., 2012 ; Wisse et al., 2014b ; Khan et al., 2014). This point is particularly important as the effect of age on brain structures is known to be non-linear, with a strong regional specificity in the dynamic of the effects (Sowell et al., 2003; Fjell et al., 2014). Moreover, most studies only investigated linear associations between age and subfield volumes, while quadratic or more complex models were used in only a few studies (Mueller et al., 2007; Ziegler et al., 2011; de Flores et al., 2015; Yang et al., 2013).

4.2. The aging subfields

Table 3 summarizes the main results from studies on the effect of age on subfield structure.

The association between hippocampal subfield integrity and age was initially evaluated in postmortem studies. West et al. (1994) described a linear effect of age on the hilus (dentate gyrus) and subiculum, with an average loss of 37% and 43% respectively from 13 to 101 years, while another study showed a linear loss of neurons for CA1 (67%) and subiculum (32%) from 16 to 99 years (Simic et al., 1997). Some researchers did not find any neuronal loss with age (Price et al., 2001; Rössler et al., 2002), probably because the age range considered was narrow, only including elderly people (60 to 89 years and 58 to 88 years, respectively).

The first *in vivo* neuroimaging study used the high-dimensional mapping method to assess shape differences between young and elder adults, showing areas of both inward (in the head and tail) and outward (in the body) deformation with increased age. Changes did not seem to be subfield-specific and rather suggested a general flattening of the whole structure (Csernansky et al. 2000). Yet, using the same method to assess longitudinal changes after a 2 year follow up in elder adults, the authors found exclusively inward surface deformations (ie. underlying tissue shrinkage) along the medial part of the hippocampus (i.e. the subiculum) and in the hippocampal head (Wang et al., 2003). Interestingly, another study found an effect on the head and subiculum with an accelerated deformation in adults over 63 years old (Yang et al., 2013). Amongst studies using radial atrophy in elderly people, two showed a global effect of age on all subfields (Wang et al., 2006; Apostolova et al., 2012), while one reported an significant effect restricted to CA1 and the presubiculum (Frisoni et al., 2008).

Using a VBM-based method, Chételat et al. (2008) found a linear association between age and the volume of the infero-medial part of the hippocampal surface mainly corresponding to the subiculum, and this result was reproduced on a different sample using the same method (La Joie et al., 2010). Thomann et al. (2012) also described a strong effect on the subiculum, as well as on the cornu ammonis (all CA subfields were grouped in the same region of interest) with a comparable method. Interestingly, Ziegler et al. (2011) used VBM with subfield probability maps (Amunts et al., 2005) on a very large sample of cognitively normal individuals (n = 547, from 19 to 86 years old) to model the dynamic of volume loss across the lifespan. They showed that the subiculum volume decreased linearly across the adult lifespan while the volume of the other subfields was approximately stable in early life, before dropping dramatically beginning around age 60.

The first subfield volumetric studies were based on manual delineation performed on the hippocampus body. Mueller et al. (2007) found a linear effect in CA1 when comparing young

to elder adults. In a subsequent study including more individuals, they also found an effect on CA3/DG (Mueller and Weiner, 2009). Another group found linear atrophy in the CA1/2 area (Shing et al., 2011; Raz et al., 2014). Kerchner et al. (2013) described a diminution of the entorhinal cortex and CA1–SRLM width in older adults compared to their younger counterparts. In other studies, the manual delineation covered almost the whole hippocampus. Thus, La Joie et al. (2010) described a linear effect of age on the subiculum with a relative preservation of CA1 and CA2/3/4/DG pooled together when considering changes in a group of individuals between 19 and 68 years old. In a follow-up study including the same 50 adults together with another 48 new individuals, de Flores et al. (2015) observed a linear decrease of the volume of the subiculum, a nonlinear decrease of CA1 volume dropping around 50 years, and no significant changes in the other subfields; this pattern of subfield atrophy dynamic across the lifespan was almost identical to the one reported by Ziegler et al (2010). In an independent sample of 29 elderly between 65 and 80 years old, Wisse et al. (2014b) reported a significant age-related volumetric decrease in CA1 and DG&CA4, with annual atrophy rates of 1.4% and 2.4%, respectively. Finally, using the automated FreeSurfer 5.3 method on a cohort of individuals between 50 and 75 years old, a recent study showed a linear effect of age on CA2/3 and CA4/DG (Pereira et al., 2014).

As mentioned above, longitudinal studies of hippocampal subfields in normal aging are rare and so far inconclusive. Das et al. (2012) showed that high-resolution structural imaging of hippocampal subfields was a viable modality for longitudinal analysis in spite of the technical complexity, partly due to voxel anisotropy of dedicated high-resolution images. Interestingly, when studying 25 cognitively normal elders, no significant longitudinal atrophy was detected in any hippocampal subfield, potentially because of the limited sample size and short follow-up duration. Moreover, Donix et al. (2010a) found that non-APOE4 carriers did

not show significant thinning in any subfield over two years whereas APOE4 carriers showed decrease in cortical thickness in all subregions except CA23-DG.

5. Cognitive correlates of subfield atrophy in aging and dementia

Although the involvement of the hippocampus in episodic memory is irrefutable, it is still unclear if and how each of its subfields potentially contributes to different aspects of memory function. Different approaches have been used to address this question, including high-resolution functional MRI (see Carr et al., 2010 for review) in healthy and impaired individuals, but also volume-cognition correlational analyses, aimed at identifying the structural correlates of inter-individual variability in cognition or the underpinnings of specific memory deficits in impaired patients.

Indeed, Mueller et al. (2011) assessed correlations between subfield volumes and two different memory scores derived from the California Verbal Learning Test (CVLT) in a mixed group including cognitively intact healthy controls with a subjective memory complaint and patients with cognitive deficits (mostly amnesic MCI patients). They showed that CA3/DG volume was related to scores assessing verbal learning and early retrieval while CA1 atrophy was correlated with impaired consolidation/delayed retrieval. Contrastingly, strong correlations were also described in AD patients between delayed recall performance and the widths of CA1-SRLM and CA1-SP, while DG/CA3 size did not significantly correlate with any aspect of memory performance (Kerchner et al., 2012). In a larger and mixed group (controls, MCI and AD patients), Kerchner et al (2014) replicated their first finding of a CA1-SRLM to delayed recall association.

Using surface-based shape or VBM-based analyses, studies have highlighted a strong association between CA1 atrophy and i) impaired free and total (free + cued) recall of verbal information in AD patients (Sarazin et al., 2010); and ii) impaired recognition performances, likely reflecting encoding deficits in amnesic MCI patients (Fouquet et al., 2012).

Accordingly, atrophy of the CA subfields (grouped together in a single region) seem to account for associative memory deficits observed in MCI patients (Atienza et al., 2011), and correlates with patients' inability to benefit from semantic processing while encoding new information. Looking at cognitive correlates of hippocampal radial atrophy, associations have been found between impaired delayed recall and CA1 and subiculum volumes in MCI (Apostolova et al., 2006b). In an equivalent analysis run on 490 individuals (including controls, MCI and AD patients from the Alzheimer's disease neuroimaging initiative), authors did not identify specific correlates in healthy controls, while areas corresponding to CA1 and subiculum were associated with delayed recall performances in MCI, and to a lesser extent in AD patients (Apostolova et al., 2010a).

A few groups have assessed memory-structure correlations in healthy controls. In healthy young adults, Chadwick et al. (2014) found that CA3 size predicted the precision of memory recall, assessed as the ability to distinguish memories with a high degree of similarity. In healthy adults between 52 and 82 years old, Bender et al. (2013) replicated a previous work (Shing et al., 2011), with larger CA3-4/dentate gyrus volume being associated with better associative memory. In this later study, CA1-2 volumes were also specifically associated with free recall of common nouns, but only in hypertensive individuals (Bender et al., 2013).

Overall, studies reporting subfield volume / memory correlations in aging and dementia have led to variable, and sometimes contradicting results. This variability is likely due to the studied samples (e.g. degree of memory impairment, whether patients and controls are pooled together, etc), but also to the important variations in both the cognitive (sub)tests and neuroimaging measurements used in the different studies. However, a couple of consistent results seem to emerge: i) the general link between CA3-4-DG volume and associative memory abilities, which is consistent with the implication of these structures in pattern separation and pattern completion (see Rolls, 2013; Yassa and Stark, 2011 for review) and, ii)

the role of CA1 atrophy in memory deficits in MCI and AD, although it is not clear whether this focal atrophy relates to specific memory components. However, these findings emanate from a limited number of labs, and are therefore derived from very specific methods (e.g. subfield definition, image acquisition, cognitive tests, etc) and need further confirmation. More generally, it is to be acknowledged that cognitive scores, especially when derived from standard clinical memory tests, do not purely reflect specific processes but should rather be seen as composite indices that combine multiple processes of memory. This notion therefore suggests one should remain cautious when interpreting these correlations between distinct memory tests and subfields.

6. Conclusion and future directions

In the present review, we gave an overview of the numerous neuroimaging approaches used to assess age- and AD-related hippocampal subfield structural changes in humans. We showed that this rapidly growing field, relying on major technical advances in terms of image acquisition and analysis, has succeeded in providing reliable *in vivo* measures of hippocampal subfields, as suggested by the similarity of the findings with neuropathological data and the progressive pattern of hippocampal subfield atrophy evidenced over the course of AD. However, some questions are still unanswered because of the limited number of studies or due to the strong contradictions between studies, especially regarding the effects of APOE4 or age on hippocampal subfields (see Table 2 and 3, respectively).

Thus, almost all studies have identified region-specific effects of pathology (at least in the earliest stages of the disease), or region-specific volume-cognition correlations, but there are strong discrepancies regarding the targeted subfield(s), most likely because of differences in the terminology and segmentation protocols used in the various laboratories working in the field. The ongoing effort for standardizing segmentation protocols led by experts in the field

gathered in the Hippocampal Subfield Group (www.hippocampalsubfields.com) is aimed at addressing these issues, and has already led to a first study comparing 21 segmentation protocols, including most of those used in the study of aging and AD (Yushkevich et al., 2015a). Interestingly, this between-protocol comparison identified the CA1/subiculum border as one of the most discrepant features among segmentation protocols. As this boundary is thought to be the earliest areas of NFT pathology within the hippocampus (Lace et al., 2009), the definition of this boundary in neuroimaging studies might have a significant impact on the detection of the subfield of greatest atrophy (i.e. CA1 or the subiculum). This protocol comparison was the first step of an effort to harmonize and enable comparisons between protocols; a white paper for harmonization has been developed (www.hippocampalsubfields.com/whitepaper) to plan for next steps (for further discussion, see Yushkevich et al., 2015a)

Moreover, while some effects have been highlighted by the vast majority of studies (e.g. CA1 atrophy in early AD), it is still uncertain what are the histological phenomena driving this macroscopic volume reduction (neuronal loss, neurite loss, neuronal shrinkage, changes in glial cells, etc?). Data from *ex vivo* MRI or *pre mortem*, *in vivo* MRI combined with histological analysis of the medial temporal lobe would highly benefit the field. The emergence of PET ligands for tau pathology (Chien et al., 2014; Maruyama et al., 2013; Okamura et al., 2014) will also allow us to question the links between hippocampal subfield atrophy and the development of tau pathology in both aging and AD. Specifically, it will give a unique opportunity to assess whether tau pathology, which appears in early/mid-life even in cognitively normal individuals (Braak and Braak, 1997; Braak and Del Tredici, 2011), underlies hippocampal subfield atrophy in both aging and dementia or whether the pattern or subfield atrophy observed in aging is independent of tau.

Lastly, hippocampus-related disorders cannot be solely studied from the interesting but narrow perspective of structural imaging, and it is certain that multimodal imaging would provide additional and complementary information on the cerebral basis of cognitive disorders (Hedden and Growdon, 2014; La Joie et al., 2014b; Maruszak and Thuret, 2014). In the coming years, the combined use of subfield-centered task-related functional MRI (Maass et al., 2014; Suthana et al., 2010; Yassa et al., 2010; see Carr et al., 2010 for review), resting-state functional MRI protocols (Das et al., 2013; Libby et al., 2012), FDG-PET (Cho et al., 2010), and diffusion tensor imaging assessing either white matter fiber tracks (Yassa et al., 2010a; Zeineh et al., 2012; Wisse et al., 2015b) or grey matter microstructure in subfields (Wolk et al., 2015) and will likely aid in understanding the multiple levels of hippocampal alteration over the course of AD (Leal and Yassa, 2013).

Acknowledgements

The authors are grateful for the financial support they have received from Association France Alzheimer ; Fondation Plan Alzheimer (Alzheimer Plan 2008–2012) ; Programme Hospitalier de Recherche Clinique (PHRC National 2011) ; Agence Nationale de la Recherche (ANR LONGVIE 2007) ; Région Basse Normandie ; Institut National de la Santé et de la Recherche Médicale (INSERM) including Ecole de l'Inserm-Liliane Bettencourt ; fondation Philippe Chatrier and fondation Thérèse et René Planiol pour l'étude du cerveau. We thank Jacob W Vogel for his comments and English editing as well as Paul Yushkevich for sharing images from his article.

References

- Aas M, Haukvik UK, Djurovic S, Tesli M, Athanasiu L, Bjella T, Hansson L, Cattaneo A, Agartz I, Andreassen O a, Melle I (2014) Interplay between childhood trauma and BDNF val66met variants on blood BDNF mRNA levels and on hippocampus subfields volumes in schizophrenia spectrum and bipolar disorders. *Journal of psychiatric research* 59:14–21.
- Adachi M, Kawakatsu S, Hosoya T, Otani K, Honma T, Shibata A, Sugai Y (2003) Morphology of the Inner Structure of the Hippocampal Formation in Alzheimer Disease. *AJNR Am J Neuroradiol* 24:1575–1581.
- Adnan A, Barnett A, Moayedi M, McCormick C, Cohn M, McAndrews MP (2015) Distinct hippocampal functional networks revealed by tractography-based parcellation. *Brain Struct Funct*.
- Aggleton JP (2012) Multiple anatomical systems embedded within the primate medial temporal lobe: implications for hippocampal function. *Neuroscience and biobehavioral reviews* 36:1579–1596.
- Albert MS, DeKosky ST, Dickson D, Dubois B, Feldman HH, Fox NC, Gamst A, Holtzman DM, Jagust WJ, Petersen RC, Snyder PJ, Carrillo MC, Thies B, Phelps CH (2011) The diagnosis of mild cognitive impairment due to Alzheimer's disease: recommendations from the National Institute on Aging-Alzheimer's Association workgroups on diagnostic guidelines for Alzheimer's disease. *Alzheimer's & dementia: the journal of the Alzheimer's Association* 7:270–279.
- Alzheimer's Association (2014) 2014 Alzheimer's disease facts and figures. *Alzheimer's & Dementia* 10:e47–e92.
- Alzheimer's Disease International (2013) *The Global Impact of Dementia 2013 – 2050*.
- Amunts K, Kedo O, Kindler M, Pieperhoff P, Mohlberg H, Shah NJ, Habel U, Schneider F, Zilles K (2005) Cytoarchitectonic mapping of the human amygdala, hippocampal region and entorhinal cortex: intersubject variability and probability maps. *Anatomy and embryology* 210:343–352.
- Apostolova LG, Dinov ID, Dutton R a, Hayashi KM, Toga AW, Cummings JL, Thompson PM (2006a) 3D comparison of hippocampal atrophy in amnesic mild cognitive impairment and Alzheimer's disease. *Brain : a journal of neurology* 129:2867–2873.
- Apostolova LG, Dutton RA, Dinov ID, Hayashi KM, Toga AW, Cummings JL, Thompson PM (2006b) Conversion of mild cognitive impairment to Alzheimer disease predicted by hippocampal atrophy maps. *Archives of neurology* 63:693–699.
- Apostolova LG, Green AE, Babakchanian S, Hwang KS, Chou Y, Toga AW, Thompson PM (2012) Hippocampal atrophy and ventricular enlargement in normal aging, mild cognitive impairment (MCI), and Alzheimer Disease. *Alzheimer disease and associated disorders* 26:17–27.

Apostolova LG, Morra JH, Green AE, Hwang KS, Avedissian C, Woo E, Cummings JL, Toga AW, Jack CR, Weiner MW, Thompson PM (2010a) Automated 3D mapping of baseline and 12-month associations between three verbal memory measures and hippocampal atrophy in 490 ADNI subjects. *NeuroImage* 51:488–499.

Apostolova LG, Mosconi L, Thompson PM, Green AE, Hwang KS, Ramirez A, Mistur R, Tsui WH, de Leon MJ (2010b) Subregional hippocampal atrophy predicts Alzheimer's dementia in the cognitively normal. *Neurobiology of aging* 31:1077–1088.

Apostolova LG, Thompson PM, Green AE, Hwang KS, Zoumalan C, Jack CR, Harvey DJ, Petersen RC, Thal LJ, Aisen PS, Toga AW, Cummings JL, Decarli CS (2010c) 3D comparison of low, intermediate, and advanced hippocampal atrophy in MCI. *Human brain mapping* 31:786–797.

Arlt S (2013) Non-Alzheimer's disease-related memory impairment and dementia. *Dialogues in clinical neuroscience* 15:465–473.

Ashburner J (2007) A fast diffeomorphic image registration algorithm. *NeuroImage* 38:95–113.

Ashburner J, Friston KJ (2000) Voxel-based morphometry--the methods. *NeuroImage* 11:805–821.

Atienza M, Atalaia-Silva KC, Gonzalez-Escamilla G, Gil-Neciga E, Suarez-Gonzalez a, Cantero JL (2011) Associative memory deficits in mild cognitive impairment: the role of hippocampal formation. *NeuroImage* 57:1331–1342.

Bender AR, Daugherty AM, Raz N (2013) Vascular risk moderates associations between hippocampal subfield volumes and memory. *Journal of cognitive neuroscience* 25:1851–1862.

Bernard C, Helmer C, Dilharreguy B, Amieva H, Auriacombe S, Dartigues J-F, Allard M, Catheline G (2014) Time course of brain volume changes in the preclinical phase of Alzheimer's disease. *Alzheimer's & dementia : the journal of the Alzheimer's Association* 10:143–151.e1.

Boccardi M et al. (2014) Delphi definition of the EADC-ADNI Harmonized Protocol for hippocampal segmentation on magnetic resonance. *Alzheimer's & dementia : the journal of the Alzheimer's Association*:1–13.

Boccardi M, Bocchetta M, Apostolova LG, Preboske G, Robitaille N, Pasqualetti P, Collins LD, Duchesne S, Jack CR, Frisoni GB (2013a) Establishing magnetic resonance images orientation for the EADC-ADNI manual hippocampal segmentation protocol. *Journal of neuroimaging : official journal of the American Society of Neuroimaging* 24:509–514.

Boccardi M, Bocchetta M, Ganzola R, Robitaille N, Redolfi A, Duchesne S, Jack CR, Frisoni GB (2013b) Operationalizing protocol differences for EADC-ADNI manual hippocampal segmentation. *Alzheimer's & dementia : the journal of the Alzheimer's Association*:1–11.

Boccardi M, Ganzola R, Bocchetta M, Pievani M, Redolfi A, Bartzokis G, Camicioli R, Csernansky JG, de Leon MJ, DeToledo-Morrell L, Killiany RJ, Lehericy S, Pantel J,

Pruessner JC, Soininen H, Watson C, Duchesne S, Jack CR, Frisoni GB (2011) Survey of protocols for the manual segmentation of the hippocampus: preparatory steps towards a joint EADC-ADNI harmonized protocol. *Journal of Alzheimer's disease* : JAD 26 Suppl 3:61–75.

Bocchetta M, Boccardi M, Ganzola R, Apostolova LG, Preboske G, Wolf D, Ferrari C, Pasqualetti P, Robitaille N, Duchesne S, Jack CR, Frisoni GB (2014) Harmonized benchmark labels of the hippocampus on magnetic resonance: The EADC-ADNI project. *Alzheimer's & dementia : the journal of the Alzheimer's Association*:1–10.

Boutet C, Chupin M, Lehéricy S, Marrakchi-Kacem L, Epelbaum S, Poupon C, Wiggins C, Vignaud A, Hasboun D, Defontaine B, Hanon O, Dubois B, Sarazin M, Hertz-Pannier L, Colliot O (2014) Detection of volume loss in hippocampal layers in Alzheimer's disease using 7 T MRI: a feasibility study. *NeuroImage: Clinical* 5:341–348.

Braak H, Braak E (1991) Neuropathological staging of Alzheimer-related changes. *Acta neuropathologica* 82:239–259.

Braak H, Braak E (1997) Diagnostic criteria for neuropathologic assessment of Alzheimer's disease. *Neurobiology of aging* 18:S85–S88.

Braak H, Braak E, Bohl J (1993) Staging of Alzheimer-related cortical destruction. *European neurology* 33:403–408.

Braak H, Del Tredici K (2011) The pathological process underlying Alzheimer's disease in individuals under thirty. *Acta neuropathologica* 121:171–181.

Brewer JB, Magda S, Airriess C, Smith ME (2009) Fully-automated quantification of regional brain volumes for improved detection of focal atrophy in Alzheimer disease. *AJNR American journal of neuroradiology* 30:578–580.

Burggren a C, Zeineh MM, Ekstrom a D, Braskie MN, Thompson PM, Small GW, Bookheimer SY (2008) Reduced cortical thickness in hippocampal subregions among cognitively normal apolipoprotein E e4 carriers. *NeuroImage* 41:1177–1183.

Burgmans S, van Boxtel MPJ, Vuurman EFPM, Smeets F, Gronenschild EHBM, Uylings HBM, Jolles J (2009) The prevalence of cortical gray matter atrophy may be overestimated in the healthy aging brain. *Neuropsychology* 23:541–550.

Carmichael O, Xie J, Fletcher E, Singh B, DeCarli C (2012) Localized hippocampus measures are associated with Alzheimer pathology and cognition independent of total hippocampal volume. *Neurobiology of aging* 33:1124.e31–e41.

Carr V a, Rissman J, Wagner AD (2010) Imaging the human medial temporal lobe with high-resolution fMRI. *Neuron* 65:298–308.

Chadwick MJ, Bonnici HM, Maguire E a (2014) CA3 size predicts the precision of memory recall. *Proceedings of the National Academy of Sciences of the United States of America* 111:10720–10725.

Chase HW, Clos M, Dibble S, Fox P, Grace AA, Phillips ML, Eickhoff SB (2015) Evidence for an anterior-posterior differentiation in the human hippocampal formation revealed by meta-analytic parcellation of fMRI coordinate maps: focus on the subiculum. *Neuroimage* 113:44–60.

Chételat G, Fouquet M, Kalpouzos G, Denghien I, De la Sayette V, Viader F, Mézenge F, Landeau B, Baron JC, Eustache F, Desgranges B (2008) Three-dimensional surface mapping of hippocampal atrophy progression from MCI to AD and over normal aging as assessed using voxel-based morphometry. *Neuropsychologia* 46:1721–1731.

Chien DT, Szardenings a K, Bahri S, Walsh JC, Mu F, Xia C, Shankle WR, Lerner AJ, Su M-Y, Elizarov A, Kolb HC (2014) Early clinical PET imaging results with the novel PHF-tau radioligand [F18]-T808. *Journal of Alzheimer's disease : JAD* 38:171–184.

Chow N, Aarsland D, Honarpisheh H, Beyer MK, Somme JH, Elashoff D, Rongve A, Tysnes OB, Thompson PM, Apostolova LG (2012) Comparing hippocampal atrophy in Alzheimer's dementia and dementia with lewy bodies. *Dementia and geriatric cognitive disorders* 34:44–50.

Chow N, Hwang KS, Hurtz S, Green AE, Somme JH, Thompson PM, Elashoff DA, Jack CR, Weiner M, Apostolova LG, Alzheimer's Disease Neuroimaging Initiative (2015) Comparing 3T and 1.5T MRI for mapping hippocampal atrophy in the Alzheimer's Disease Neuroimaging Initiative. *AJNR Am J Neuroradiol* 36:653–660.

Cho Z-H, Son Y-D, Kim H-K, Kim S-T, Lee S-Y, Chi J-G, Park C-W, Kim Y-B (2010) Substructural hippocampal glucose metabolism observed on PET/MRI. *Journal of nuclear medicine : official publication, Society of Nuclear Medicine* 51:1545–1548.

Chupin M, Hammers a, Liu RSN, Colliot O, Burdett J, Bardinet E, Duncan JS, Garnero L, Lemieux L (2009) Automatic segmentation of the hippocampus and the amygdala driven by hybrid constraints: method and validation. *NeuroImage* 46:749–761.

Corder EH, Saunders AM, Strittmatter WJ, Schmechel DE, Gaskell PC, Small GW, Roses AD, Haines JL, Pericak-Vance MA (1993) Gene dose of apolipoprotein E type 4 allele and the risk of Alzheimer's disease in late onset families. *Science (New York, NY)* 261:921–923.

Csernansky JG, Wang L, Joshi S, Miller JP, Gado M, Kido D, McKeel D, Morris JC, Miller MI (2000) Early DAT is distinguished from aging by high-dimensional mapping of the hippocampus. *Dementia of the Alzheimer type. Neurology* 55:1636–1643.

Csernansky JG, Wang L, Swank J, Miller JP, Gado M, McKeel D, Miller MI, Morris JC (2005) Preclinical detection of Alzheimer's disease: hippocampal shape and volume predict dementia onset in the elderly. *NeuroImage* 25:783–792.

Das SR, Avants BB, Pluta J, Wang H, Suh JW, Weiner MW, Mueller SG, Yushkevich P a (2012) Measuring longitudinal change in the hippocampal formation from in vivo high-resolution T2-weighted MRI. *NeuroImage* 60:1266–1279.

Das SR, Pluta J, Mancuso L, Kliot D, Orozco S, Dickerson BC, Yushkevich P a, Wolk D a (2013) Increased functional connectivity within medial temporal lobe in mild cognitive impairment. *Hippocampus* 23:1–6.

de Flores R, La Joie R, Landeau B, Perrotin A, Mézenge F, de La Sayette V, Eustache F, Desgranges B, Chételat G (2015) Effects of age and Alzheimer's disease on hippocampal subfields: comparison between manual and FreeSurfer volumetry. *Human brain mapping* 36:463–474.

Dill V, Franco AR, Pinho MS (2014) Automated Methods for Hippocampus Segmentation: the Evolution and a Review of the State of the Art. *Neuroinformatics*.

DiLuca M, Olesen J (2014) The cost of brain diseases: a burden or a challenge? *Neuron* 82:1205–1208.

Donix M, Burggren AC, Suthana NA, Siddarth P, Ekstrom AD, Krupa AK, Jones M, Martin-Harris L, Ercoli LM, Miller KJ, Small GW, Bookheimer SY (2010a) Family history of Alzheimer's disease and hippocampal structure in healthy people. *The American journal of psychiatry* 167:1399–1406.

Donix M, Burggren AC, Suthana N a, Siddarth P, Ekstrom AD, Krupa AK, Jones M, Rao A, Martin-Harris L, Ercoli LM, Miller KJ, Small GW, Bookheimer SY (2010b) Longitudinal changes in medial temporal cortical thickness in normal subjects with the APOE-4 polymorphism. *NeuroImage* 53:37–43.

Doraiswamy PM, Sperling R a, Johnson K, Reiman EM, Wong TZ, Sabbagh MN, Sadowsky CH, Fleisher a S, Carpenter a, Joshi a D, Lu M, Grundman M, Mintun M a, Skovronsky DM, Pontecorvo MJ (2014) Florbetapir F 18 amyloid PET and 36-month cognitive decline: a prospective multicenter study. *Molecular psychiatry* 19:1044–1051.

Dotson VM, Davatzikos C, Kraut MA, Resnick SM (2009) Depressive symptoms and brain volumes in older adults: a longitudinal magnetic resonance imaging study. *Journal of psychiatry & neuroscience : JPN* 34:367–375.

Driscoll I, Davatzikos C, An Y, Wu X, Shen D, Kraut M, Resnick SM (2009) Longitudinal pattern of regional brain volume change differentiates normal aging from MCI. *Neurology* 72:1906–1913.

Driscoll I, Hamilton DA, Petropoulos H, Yeo RA, Brooks WM, Baumgartner RN, Sutherland RJ (2003) The aging hippocampus: cognitive, biochemical and structural findings. *Cerebral cortex (New York, NY : 1991)* 13:1344–1351.

Dubois B et al. (2010) Revising the definition of Alzheimer's disease: a new lexicon. *Lancet neurology* 9:1118–1127.

Dubois B et al. (2014) Advancing research diagnostic criteria for Alzheimer's disease: the IWG-2 criteria. *Lancet neurology* 13:614–629.

Dubois B, Feldman HH, Jacova C, Dekosky ST, Barberger-Gateau P, Cummings J, Delacourte A, Galasko D, Gauthier S, Jicha G, Meguro K, O'brien J, Pasquier F, Robert P, Rossor M, Salloway S, Stern Y, Visser PJ, Scheltens P (2007) Research criteria for the

diagnosis of Alzheimer's disease: revising the NINCDS-ADRDA criteria. *Lancet neurology* 6:734–746.

Durazzo TC, Meyerhoff DJ, Nixon SJ (2013) Interactive effects of chronic cigarette smoking and age on hippocampal volumes. *Drug and alcohol dependence* 133:704–711.

Duvernoy HM (2005) *The Human Hippocampus, Functional Anatomy, Vascularization and Serial Sections with MRI*, Third edit. Berlin, Germany: Springer-Verlag.

Duyckaerts C, Delatour B, Potier M-C (2009) Classification and basic pathology of Alzheimer disease. *Acta neuropathologica* 118:5–36.

Ekstrom AD, Bazih AJ, Suthana N a, Al-Hakim R, Ogura K, Zeineh M, Burggren AC, Bookheimer SY (2009) Advances in high-resolution imaging and computational unfolding of the human hippocampus. *NeuroImage* 47:42–49.

El-Falougy H, Benuska J (2006) History, anatomical nomenclature, comparative anatomy and functions of the hippocampal formation. *Bratislavské lekárske listy* 107:103–106.

Engvig A, Fjell AM, Westlye LT, Skaane N V, Sundseth Ø, Walhovd KB (2012) Hippocampal subfield volumes correlate with memory training benefit in subjective memory impairment. *NeuroImage* 61:188–194.

Ezzati A, Zimmerman ME, Katz MJ, Sundermann EE, Smith JL, Lipton ML, Lipton RB (2014) Hippocampal subfields differentially correlate with chronic pain in older adults. *Brain research* 1573:54–62.

Farrer LA, Cupples LA, Haines JL, Hyman B, Kukull WA, Mayeux R, Myers RH, Pericak-Vance MA, Risch N, van Duijn CM (1997) Effects of age, sex, and ethnicity on the association between apolipoprotein E genotype and Alzheimer disease. A meta-analysis. APOE and Alzheimer Disease Meta Analysis Consortium. *JAMA* 278:1349–1356.

Fischl B, Salat DH, Busa E, Albert M, Dieterich M, Haselgrove C, van der Kouwe A, Killiany R, Kennedy D, Klaveness S, Montillo A, Makris N, Rosen B, Dale AM (2002) Whole brain segmentation: automated labeling of neuroanatomical structures in the human brain. *Neuron* 33:341–355.

Fjell AM, McEvoy L, Holland D, Dale AM, Walhovd KB (2014a) What is normal in normal aging? Effects of aging, amyloid and Alzheimer's disease on the cerebral cortex and the hippocampus. *Progress in neurobiology* 117:20–40.

Fjell AM, Walhovd KB (2010) Structural brain changes in aging: courses, causes and cognitive consequences. *Reviews in the neurosciences* 21:187–221.

Fjell AM, Walhovd KB, Fennema-Notestine C, McEvoy LK, Hagler DJ, Holland D, Brewer JB, Dale AM (2009) One-year brain atrophy evident in healthy aging. *The Journal of neuroscience : the official journal of the Society for Neuroscience* 29:15223–15231.

Fjell AM, Westlye LT, Grydeland H, Amlien I, Espeseth T, Reinvang I, Raz N, Dale AM, Walhovd KB (2014b) Accelerating cortical thinning: unique to dementia or universal in aging? *Cerebral cortex (New York, NY : 1991)* 24:919–934.

Fotuhi M, Do D, Jack C (2012) Modifiable factors that alter the size of the hippocampus with ageing. *Nature reviews Neurology* 8:189–202.

Fouquet M, Besson FL, Gonneaud J, La Joie R, Chételat G (2014) Imaging brain effects of APOE4 in cognitively normal individuals across the lifespan. *Neuropsychology review* 24:290–299.

Fouquet M, Desgranges B, La Joie R, Rivière D, Mangin J-F, Landeau B, Mézange F, Pélerin A, de La Sayette V, Viader F, Baron J-C, Eustache F, Chételat G (2012) Role of hippocampal CA1 atrophy in memory encoding deficits in amnesic Mild Cognitive Impairment. *NeuroImage* 59:3309–3315.

Francis AN, Seidman LJ, Tandon N, Shenton ME, Thermenos HW, Mesholam-Gately RI, van Elst LT, Tuschen-Caffier B, DeLisi LE, Keshavan MS (2013) Reduced subicular subdivisions of the hippocampal formation and verbal declarative memory impairments in young relatives at risk for schizophrenia. *Schizophrenia research* 151:154–157.

Frisoni GB et al. (2014) The EADC-ADNI Harmonized Protocol for manual hippocampal segmentation on magnetic resonance: Evidence of validity. *Alzheimer's & dementia : the journal of the Alzheimer's Association*:1–15.

Frisoni GB, Fox NC, Jack CR, Scheltens P, Thompson PM (2010) The clinical use of structural MRI in Alzheimer disease. *Nature reviews Neurology* 6:67–77.

Frisoni GB, Ganzola R, Canu E, Rüb U, Pizzini FB, Alessandrini F, Zoccatelli G, Beltramello A, Caltagirone C, Thompson PM (2008) Mapping local hippocampal changes in Alzheimer's disease and normal ageing with MRI at 3 Tesla. *Brain: a journal of neurology* 131:3266–3276.

Frisoni GB, Sabattoli F, Lee a D, Dutton R a, Toga a W, Thompson PM (2006) In vivo neuropathology of the hippocampal formation in AD: a radial mapping MR-based study. *NeuroImage* 32:104–110.

Fukutani Y, Cairns NJ, Shiozawa M, Sasaki K, Sudo S, Isaki K, Lantos PL (2000) Neuronal loss and neurofibrillary degeneration in the hippocampal cortex in late-onset sporadic Alzheimer's disease. *Psychiatry and clinical neurosciences* 54:523–529.

Ganguli M, Snitz BE, Saxton JA, Chang C-CH, Lee C-W, Vander Bilt J, Hughes TF, Loewenstein DA, Unverzagt FW, Petersen RC (2011) Outcomes of mild cognitive impairment by definition: a population study. *Archives of neurology* 68:761–767.

Gemmell E, Bosomworth H, Allan L, Hall R, Khundakar A, Oakley AE, Deramecourt V, Polvikoski TM, O'Brien JT, Kalaria RN (2012) Hippocampal neuronal atrophy and cognitive function in delayed poststroke and aging-related dementias. *Stroke; a journal of cerebral circulation* 43:808–814.

Genin E et al. (2011) APOE and Alzheimer disease: a major gene with semi-dominant inheritance. *Molecular psychiatry* 16:903–907.

Gerardin E, Chételat G, Chupin M, Cuingnet R, Desgranges B, Kim H-S, Niethammer M, Dubois B, Lehéricy S, Garnero L, Eustache F, Colliot O (2009) Multidimensional

classification of hippocampal shape features discriminates Alzheimer's disease and mild cognitive impairment from normal aging. *NeuroImage* 47:1476–1486.

Geuze E, Vermetten E, Bremner JD (2005a) MR-based in vivo hippocampal volumetrics: 2. Findings in neuropsychiatric disorders. *Molecular psychiatry* 10:160–184.

Geuze E, Vermetten E, Bremner JD (2005b) MR-based in vivo hippocampal volumetrics: 1. Review of methodologies currently employed. *Molecular psychiatry* 10:147–159.

Gordon B a, Blazey T, Benzinger TLS, Head D (2013) Effects of aging and Alzheimer's disease along the longitudinal axis of the hippocampus. *Journal of Alzheimer's disease : JAD* 37:41–50.

Hanseeuw BJ, Van Leemput K, Kavec M, Grandin C, Seron X, Ivanoiu A (2011) Mild cognitive impairment: differential atrophy in the hippocampal subfields. *AJNR American journal of neuroradiology* 32:1658–1661.

Haukvik UK, Westlye LT, Mørch-Johnsen L, Jørgensen KN, Lange EH, Dale AM, Melle I, Andreassen O a, Agartz I (2014) In Vivo Hippocampal Subfield Volumes in Schizophrenia and Bipolar Disorder. *Biological psychiatry*:1–8.

Hedden T, Growdon JH (2014) Challenges and Opportunities in Linking Brain-Based Biomarkers to Person-Specific Variation in Cognition: Pumping Up the Volume. *JAMA neurology*.

Hsu PJ, Shu H, Benzinger T, Marcus D, Durbin T, Morris JC, Sheline YI (2014) Amyloid Burden in Cognitively Normal Elderly is Associated with Preferential Hippocampal Subfield Volume Loss. *Journal of Alzheimer's disease : JAD* L:1–7.

Huang Y, Coupland NJ, Lebel RM, Carter R, Seres P, Wilman AH, Malykhin N V (2013) Structural changes in hippocampal subfields in major depressive disorder: a high-field magnetic resonance imaging study. *Biological psychiatry* 74:62–68.

Hughes TF, Snitz BE, Ganguli M (2011) Should mild cognitive impairment be subtyped? *Current opinion in psychiatry* 24:237–242.

Hyman BT, Phelps CH, Beach TG, Bigio EH, Cairns NJ, Carrillo MC, Dickson DW, Duyckaerts C, Frosch MP, Masliah E, Mirra SS, Nelson PT, Schneider J a, Thal DR, Thies B, Trojanowski JQ, Vinters H V, Montine TJ (2012) National Institute on Aging-Alzheimer's Association guidelines for the neuropathologic assessment of Alzheimer's disease. *Alzheimer's & dementia : the journal of the Alzheimer's Association* 8:1–13.

Iglesias JE, Augustinack JC, Nguyen K, Player CM, Player A, Wright M, Roy N, Frosch MP, McKee AC, Wald LL, Fischl B, Van Leemput K, Alzheimer's Disease Neuroimaging Initiative (2015) A computational atlas of the hippocampal formation using ex vivo, ultra-high resolution MRI: Application to adaptive segmentation of in vivo MRI. *Neuroimage* 115:117–137.

Jack CR, Petersen RC, Xu YC, Waring SC, O'Brien PC, Tangalos EG, Smith GE, Ivnik RJ, Kokmen E (1997) Medial temporal atrophy on MRI in normal aging and very mild Alzheimer's disease. *Neurology* 49:786–794.

Jack CR, Vemuri P, Wiste HJ, Weigand SD, Lesnick TG, Lowe V, Kantarci K, Bernstein M a, Senjem ML, Gunter JL, Boeve BF, Trojanowski JQ, Shaw LM, Aisen PS, Weiner MW, Petersen RC, Knopman DS (2012) Shapes of the trajectories of 5 major biomarkers of Alzheimer disease. *Archives of neurology* 69:856–867.

Jessen F, Wolfsgruber S, Wiese B, Bickel H, Mösch E, Kaduszkiewicz H, Pentzek M, Riedel-Heller SG, Luck T, Fuchs A, Weyerer S, Werle J, van den Bussche H, Scherer M, Maier W, Wagner M (2014) AD dementia risk in late MCI, in early MCI, and in subjective memory impairment. *Alzheimer's & dementia : the journal of the Alzheimer's Association* 10:76–83.

Kerchner GA, Berdnik D, Shen JC, Bernstein JD, Fenesy MC, Deutsch GK, Wyss-Coray T, Rutt BK (2014) APOE ϵ 4 worsens hippocampal CA1 apical neuropil atrophy and episodic memory. *Neurology* 82:691–697.

Kerchner GA, Bernstein JD, Fenesy MC, Deutsch GK, Saranathan M, Zeineh MM, Rutt BK (2013) Shared vulnerability of two synaptically-connected medial temporal lobe areas to age and cognitive decline: a seven tesla magnetic resonance imaging study. *The Journal of neuroscience : the official journal of the Society for Neuroscience* 33:16666–16672.

Kerchner G a, Deutsch GK, Zeineh M, Dougherty RF, Saranathan M, Rutt BK (2012) Hippocampal CA1 apical neuropil atrophy and memory performance in Alzheimer's disease. *NeuroImage* 63:194–202.

Kerchner GA, Hess CP, Hammond-Rosenbluth KE, Xu D, Rabinovici GD, Kelley DAC, Vigneron DB, Nelson SJ, Miller BL (2010) Hippocampal CA1 apical neuropil atrophy in mild Alzheimer disease visualized with 7-T MRI. *Neurology* 75:1381–1387.

Khachaturian ZS (1985) Diagnosis of Alzheimer's disease. *Archives of neurology* 42:1097–1105.

Khan W, Westman E, Jones N, Wahlund L-O, Mecocci P, Vellas B, Tsolaki M, Kłoszewska I, Soininen H, Spenger C, Lovestone S, Muehlboeck J-S, Simmons A (2014) Automated Hippocampal Subfield Measures as Predictors of Conversion from Mild Cognitive Impairment to Alzheimer's Disease in Two Independent Cohorts. *Brain topography*.

Knopman DS, Jack CR, Wiste HJ, Weigand SD, Vemuri P, Lowe V, Kantarci K, Gunter JL, Senjem ML, Ivnik RJ, Roberts RO, Boeve BF, Petersen RC (2012) Short-term clinical outcomes for stages of NIA-AA preclinical Alzheimer disease. *Neurology* 78:1576–1582.

Koepsell TD, Monsell SE (2012) Reversion from mild cognitive impairment to normal or near-normal cognition: risk factors and prognosis. *Neurology* 79:1591–1598.

Konrad C, Ukas T, Nebel C, Arolt V, Toga a W, Narr KL (2009) Defining the human hippocampus in cerebral magnetic resonance images--an overview of current segmentation protocols. *NeuroImage* 47:1185–1195.

Kril JJ, Patel S, Harding AJ, Halliday GM (2002) Patients with vascular dementia due to microvascular pathology have significant hippocampal neuronal loss. *Journal of neurology, neurosurgery, and psychiatry* 72:747–751.

Krogsrud SK, Tamnes CK, Fjell AM, Amlien I, Grydeland H, Sulutvedt U, Due-Tønnessen P, Bjørnerud A, Sølsnes AE, Håberg AK, Skrane J, Walhovd KB (2014) Development of hippocampal subfield volumes from 4 to 22 years. *Human brain mapping* 35:5646–5657.

Kühn S, Charlet K, Schubert F, Kiefer F, Zimmermann P, Heinz A, Gallinat J (2014) Plasticity of hippocampal subfield volume cornu ammonis 2+3 over the course of withdrawal in patients with alcohol dependence. *JAMA psychiatry* 71:806–811.

Lace G, Savva GM, Forster G, de Silva R, Brayne C, Matthews FE, Barclay JJ, Dakin L, Ince PG, Wharton SB (2009) Hippocampal tau pathology is related to neuroanatomical connections: an ageing population-based study. *Brain : a journal of neurology* 132:1324–1334.

La Joie R, Fouquet M, Mézenge F, Landeau B, Villain N, Mevel K, Pélerin A, Eustache F, Desgranges B, Chételat G (2010) Differential effect of age on hippocampal subfields assessed using a new high-resolution 3T MR sequence. *NeuroImage* 53:506–514.

La Joie R, Landeau B, Perrotin A, Bejanin A, Egret S, Pélerin A, Mézenge F, Belliard S, de La Sayette V, Eustache F, Desgranges B, Chételat G (2014a) Intrinsic connectivity identifies the hippocampus as a main crossroad between Alzheimer's and semantic dementia-targeted networks. *Neuron* 81:1417–1428.

La Joie R, Perrotin A, de La Sayette V, Egret S, Doeuvre L, Belliard S, Eustache F, Desgranges B, Chételat G (2013) Hippocampal subfield volumetry in mild cognitive impairment, Alzheimer's disease and semantic dementia. *NeuroImage Clinical* 3:155–162.

La Joie R (2014b). Toward a better understanding of the injured hippocampus: multimodal imaging in functionally relevant substructures. *The Journal of neuroscience : the official journal of the Society for Neuroscience* 34: 10793-4

Leal SL, Yassa M a (2013) Perturbations of neural circuitry in aging, mild cognitive impairment, and Alzheimer's disease. *Ageing research reviews* 12:823–831.

Leung KK, Barnes J, Ridgway GR, Bartlett JW, Clarkson MJ, Macdonald K, Schuff N, Fox NC, Ourselin S (2010) Automated cross-sectional and longitudinal hippocampal volume measurement in mild cognitive impairment and Alzheimer's disease. *NeuroImage* 51:1345–1359.

Libby LA, Ekstrom AD, Ragland JD, Ranganath C (2012) Differential connectivity of perirhinal and parahippocampal cortices within human hippocampal subregions revealed by high-resolution functional imaging. *The Journal of neuroscience : the official journal of the Society for Neuroscience* 32:6550–6560.

Lim HK, Hong SC, Jung WS, Ahn KJ, Won WY, Hahn C, Kim I, Lee CU (2012a) Automated hippocampal subfields segmentation in late life depression. *Journal of affective disorders* 143:253–256.

Lim HK, Hong SC, Jung WS, Ahn KJ, Won WY, Hahn C, Kim IS, Lee CU (2012b) Automated hippocampal subfield segmentation in amnesic mild cognitive impairments. *Dementia and geriatric cognitive disorders* 33:327–333.

Lindberg O, Walterfang M, Looi JCL, Malykhin N, Ostberg P, Zandbelt B, Styner M, Paniagua B, Velakoulis D, Orndahl E, Wahlund L-O (2012) Hippocampal shape analysis in Alzheimer's disease and frontotemporal lobar degeneration subtypes. *Journal of Alzheimer's disease : JAD* 30:355–365.

Li Y-D, Dong H-B, Xie G-M, Zhang L (2013) Discriminative analysis of mild Alzheimer's disease and normal aging using volume of hippocampal subfields and hippocampal mean diffusivity: an in vivo magnetic resonance imaging study. *American journal of Alzheimer's disease and other dementias* 28:627–633.

Lockhart SN, DeCarli C (2014) Structural imaging measures of brain aging. *Neuropsychology review* 24:271–289.

Maass A, Schütze H, Speck O, Yonelinas A, Tempelmann C, Heinze H-J, Berron D, Cardenas-Blanco A, Brodersen KH, Enno Stephan K, Düzel E (2014) Laminar activity in the hippocampus and entorhinal cortex related to novelty and episodic encoding. *Nature communications* 5:5547.

Malykhin N V, Bouchard TP, Camicioli R, Coupland NJ (2008) Aging hippocampus and amygdala. *Neuroreport* 19:543–547.

Marcus DS, Fotenos AF, Csernansky JG, Morris JC, Buckner RL (2010) Open access series of imaging studies: longitudinal MRI data in nondemented and demented older adults. *Journal of cognitive neuroscience* 22:2677–2684.

Markesbery WR (1997) Neuropathological criteria for the diagnosis of Alzheimer's disease. *Neurobiology of aging* 18:S13–S19.

Maruszak A, Thuret S (2014) Why looking at the whole hippocampus is not enough—a critical role for anteroposterior axis, subfield and activation analyses to enhance predictive value of hippocampal changes for Alzheimer's disease diagnosis. *Frontiers in cellular neuroscience* 8:95.

Maruyama M et al. (2013) Imaging of tau pathology in a tauopathy mouse model and in Alzheimer patients compared to normal controls. *Neuron* 79:1094–1108.

McKhann G, Drachman D, Folstein M, Katzman R, Price D, Stadlan EM (1984) Clinical diagnosis of Alzheimer's disease: Report of the NINCDS-ADRDA Work Group* under the auspices of Department of Health and Human Services Task Force on Alzheimer's Disease. *Neurology* 34:939–939.

McKhann GM, Knopman DS, Chertkow H, Hyman BT, Jack CR, Kawas CH, Klunk WE, Koroshetz WJ, Manly JJ, Mayeux R, Mohs RC, Morris JC, Rossor MN, Scheltens P, Carrillo MC, Thies B, Weintraub S, Phelps CH (2011) The diagnosis of dementia due to Alzheimer's disease: recommendations from the National Institute on Aging-Alzheimer's Association workgroups on diagnostic guidelines for Alzheimer's disease. *Alzheimer's & dementia : the journal of the Alzheimer's Association* 7:263–269.

Mirra SS, Heyman A, McKeel D, Sumi SM, Crain BJ, Brownlee LM, Vogel FS, Hughes JP, van Belle G, Berg L (1991) The Consortium to Establish a Registry for Alzheimer's Disease (CERAD). Part II. Standardization of the neuropathologic assessment of Alzheimer's disease. *Neurology* 41:479–486.

Mitchell a J, Shiri-Feshki M (2009) Rate of progression of mild cognitive impairment to dementia--meta-analysis of 41 robust inception cohort studies. *Acta psychiatrica Scandinavica* 119:252–265.

Montine TJ, Phelps CH, Beach TG, Bigio EH, Cairns NJ, Dickson DW, Duyckaerts C, Frosch MP, Masliah E, Mirra SS, Nelson PT, Schneider J a, Thal DR, Trojanowski JQ, Vinters H V, Hyman BT (2012) National Institute on Aging-Alzheimer's Association guidelines for the neuropathologic assessment of Alzheimer's disease: a practical approach. *Acta neuropathologica* 123:1–11.

Morra JH, Tu Z, Apostolova LG, Green AE, Avedissian C, Madsen SK, Parikshak N, Hua X, Toga AW, Jack CR, Weiner MW, Thompson PM (2008) Validation of a fully automated 3D hippocampal segmentation method using subjects with Alzheimer's disease mild cognitive impairment, and elderly controls. *NeuroImage* 43:59–68.

Mueller SG, Schuff N, Raptentsetsang S, Elman J, Weiner MW (2008) Selective effect of Apo e4 on CA3 and dentate in normal aging and Alzheimer's disease using high resolution MRI at 4 T. *NeuroImage* 42:42–48.

Mueller SG, Schuff N, Yaffe K, Madison C, Miller B, Weiner MW (2010) Hippocampal atrophy patterns in mild cognitive impairment and Alzheimer's disease. *Human brain mapping* 31:1339–1347.

Mueller SG, Stables L, Du AT, Schuff N, Truran D, Cashdollar N, Weiner MW (2007) Measurement of hippocampal subfields and age-related changes with high resolution MRI at 4T. *Neurobiology of aging* 28:719–726.

Mueller SG, Weiner MW (2009) Selective effect of age, Apo e4, and Alzheimer's disease on hippocampal subfields. *Hippocampus* 19:558–564.

Mueller SG, Weiner MW, Thal LJ, Petersen RC, Jack CR, Jagust W, Trojanowski JQ, Toga AW, Beckett L (2005) Ways toward an early diagnosis in Alzheimer's disease: the Alzheimer's Disease Neuroimaging Initiative (ADNI). *Alzheimer's & dementia: the journal of the Alzheimer's Association* 1:55–66.

Okamura N, Furumoto S, Fodero-Tavoletti MT, Mulligan RS, Harada R, Yates P, Pejoska S, Kudo Y, Masters CL, Yanai K, Rowe CC, Villemagne VL (2014) Non-invasive assessment of Alzheimer's disease neurofibrillary pathology using 18F-THK5105 PET. *Brain: a journal of neurology* 137:1762–1771.

Padurariu M, Ciobica A, Mavroudis I, Fotiou D, Baloyannis S (2012) HIPPOCAMPAL NEURONAL LOSS IN THE CA1 AND CA3 AREAS OF ALZHEIMER ' S DISEASE PATIENTS. *24:152–158.*

Patenaude B, Smith SM, Kennedy DN, Jenkinson M (2011) A Bayesian model of shape and appearance for subcortical brain segmentation. *NeuroImage* 56:907–922.

Pereira JB, Junqué C, Bartrés-Faz D, Ramírez-Ruiz B, Martí M-J, Tolosa E (2013) Regional vulnerability of hippocampal subfields and memory deficits in Parkinson's disease. *Hippocampus* 23:720–728.

Pereira JB, Valls-Pedret C, Ros E, Palacios E, Falcón C, Bargalló N, Bartrés-Faz D, Wahlund L-O, Westman E, Junqué C (2014) Regional vulnerability of hippocampal subfields to aging measured by structural and diffusion MRI. *Hippocampus* 24:403–414.

Pfefferbaum A, Sullivan EV (2015) Cross-sectional versus longitudinal estimates of age-related changes in the adult brain: overlaps and discrepancies. *Neurobiol Aging* 36:2563–2567.

Pipitone J, Park MTM, Winterburn J, Lett T a, Lerch JP, Pruessner JC, Lepage M, Voineskos AN, Chakravarty MM (2014) Multi-atlas segmentation of the whole hippocampus and subfields using multiple automatically generated templates. *NeuroImage* 101:494–512.

Pluta J, Yushkevich P, Das S, Wolk D (2012) In vivo analysis of hippocampal subfield atrophy in mild cognitive impairment via semi-automatic segmentation of T2-weighted MRI. *Journal of Alzheimer's disease* 31:85–99.

Poppenk J, Evensmoen HR, Moscovitch M, Nadel L (2013) Long-axis specialization of the human hippocampus. *Trends in cognitive sciences* 17:230–240.

Price JL, Ko a I, Wade MJ, Tsou SK, McKeel DW, Morris JC (2001) Neuron number in the entorhinal cortex and CA1 in preclinical Alzheimer disease. *Archives of neurology* 58:1395–1402.

Raz N, Daugherty AM, Bender AR, Dahle CL, Land S (2014) Volume of the hippocampal subfields in healthy adults: differential associations with age and a pro-inflammatory genetic variant. *Brain structure & function*.

Raz N, Lindenberger U, Rodrigue KM, Kennedy KM, Head D, Williamson A, Dahle C, Gerstorff D, Acker JD (2005) Regional brain changes in aging healthy adults: general trends, individual differences and modifiers. *Cerebral cortex (New York, NY : 1991)* 15:1676–1689.

Raz N, Rodrigue KM (2006) Differential aging of the brain: patterns, cognitive correlates and modifiers. *Neuroscience and biobehavioral reviews* 30:730–748.

Raz N, Rodrigue KM, Head D, Kennedy KM, Acker JD (2004) Differential aging of the medial temporal lobe: a study of a five-year change. *Neurology* 62:433–438.

Resnick SM, Pham DL, Kraut MA, Zonderman AB, Davatzikos C (2003) Longitudinal magnetic resonance imaging studies of older adults: a shrinking brain. *The Journal of neuroscience : the official journal of the Society for Neuroscience* 23:3295–3301.

Rolls ET (2013) The mechanisms for pattern completion and pattern separation in the hippocampus. *Frontiers in systems neuroscience* 7:74.

Rossi R, Lanfredi M, Pievani M, Boccardi M, Beneduce R, Rilloso L, Giannakopoulos P, Thompson PM, Rossi G, Frisoni GB (2012) Volumetric and topographic differences in

hippocampal subdivisions in borderline personality and bipolar disorders. *Psychiatry research* 203:132–138.

Rössler M, Zarski R, Bohl J, Ohm TG (2002) Stage-dependent and sector-specific neuronal loss in hippocampus during Alzheimer's disease. *Acta neuropathologica* 103:363–369.

Sabattoli F, Boccardi M, Galluzzi S, Treves a, Thompson PM, Frisoni GB (2008) Hippocampal shape differences in dementia with Lewy bodies. *NeuroImage* 41:699–705.

Sarazin M, Chauviré V, Gerardin E, Colliot O, Kinkingnéhun S, de Souza LC, Hugonot-Diener L, Garnero L, Lehericy S, Chupin M, Dubois B (2010) The amnesic syndrome of hippocampal type in Alzheimer's disease: an MRI study. *Journal of Alzheimer's disease : JAD* 22:285–294.

Scahill RI, Frost C, Jenkins R, Whitwell JL, Rossor MN, Fox NC (2003) A longitudinal study of brain volume changes in normal aging using serial registered magnetic resonance imaging. *Archives of neurology* 60:989–994.

Scher a I, Xu Y, Korf ESC, White LR, Scheltens P, Toga a W, Thompson PM, Hartley SW, Witter MP, Valentino DJ, Launer LJ (2007) Hippocampal shape analysis in Alzheimer's disease: a population-based study. *NeuroImage* 36:8–18.

Schönheit B, Zarski R, Ohm TG (2004) Spatial and temporal relationships between plaques and tangles in Alzheimer-pathology. *Neurobiology of aging* 25:697–711.

Schultz C, Engelhardt M (2014) Anatomy of the hippocampal formation. *Front Neurol Neurosci* 34:6–17.

Scoville WB, Milner B (1957) Loss of recent memory after bilateral hippocampal lesions. *Journal of neurology, neurosurgery, and psychiatry* 20:11–21.

Seab JP, Jagust WJ, Wong ST, Roos MS, Reed BR, Budinger TF (1988) Quantitative NMR measurements of hippocampal atrophy in Alzheimer's disease. *Magnetic resonance in medicine : official journal of the Society of Magnetic Resonance in Medicine / Society of Magnetic Resonance in Medicine* 8:200–208.

Shi F, Liu B, Zhou Y, Yu C, Jiang T (2009) Hippocampal volume and asymmetry in mild cognitive impairment and Alzheimer's disease: Meta-analyses of MRI studies. *Hippocampus* 19:1055–1064.

Shing YL, Rodrigue KM, Kennedy KM, Fandakova Y, Bodammer N, Werkle-Bergner M, Lindenberger U, Raz N (2011) Hippocampal subfield volumes: age, vascular risk, and correlation with associative memory. *Frontiers in aging neuroscience* 3:2.

Sicotte NL, Kern KC, Giesser BS, Arshanapalli a, Schultz a, Montag M, Wang H, Bookheimer SY (2008) Regional hippocampal atrophy in multiple sclerosis. *Brain : a journal of neurology* 131:1134–1141.

Simic G, Kostovic I, Winblad B, Bogdanovic N (1997) Volume and number of neurons of the human hippocampal formation in normal aging and Alzheimer's disease. *Journal of Comparative neurology* 379:482–494.

Small S a, Schobel S a, Buxton RB, Witter MP, Barnes C a (2011) A pathophysiological framework of hippocampal dysfunction in ageing and disease. *Nature reviews Neuroscience* 12:585–601.

Smith CD, Andersen AH, Gold BT (2012) Structural brain alterations before mild cognitive impairment in ADNI: validation of volume loss in a predefined antero-temporal region. *Journal of Alzheimer's disease : JAD* 31 Suppl 3:S49–S58.

Smith CD, Chebrolu H, Wekstein DR, Schmitt FA, Jicha GA, Cooper G, Markesbery WR (2007) Brain structural alterations before mild cognitive impairment. *Neurology* 68:1268–1273.

Sowell ER, Peterson BS, Thompson PM, Welcome SE, Henkenius AL, Toga AW (2003) Mapping cortical change across the human life span. *Nature neuroscience* 6:309–315.

Spaniol J, Davidson PSR, Kim ASN, Han H, Moscovitch M, Grady CL (2009) Event-related fMRI studies of episodic encoding and retrieval: meta-analyses using activation likelihood estimation. *Neuropsychologia* 47:1765–1779.

Sperling RA et al. (2011) Toward defining the preclinical stages of Alzheimer's disease: recommendations from the National Institute on Aging-Alzheimer's Association workgroups on diagnostic guidelines for Alzheimer's disease. *Alzheimer's & dementia : the journal of the Alzheimer's Association* 7:280–292.

Squire LR (2009) The legacy of patient H.M. for neuroscience. *Neuron* 61:6–9.

Squire LR, Ojemann JG, Miezin FM, Petersen SE, Videen TO, Raichle ME (1992) Activation of the hippocampus in normal humans: a functional anatomical study of memory. *Proceedings of the National Academy of Sciences of the United States of America* 89:1837–1841.

Suppa P, Anker U, Spies L, Bopp I, Rügger-Frey B, Klaghofer R, Gocke C, Hampel H, Beck S, Buchert R (2015a) Fully automated atlas-based hippocampal volumetry for detection of Alzheimer's disease in a memory clinic setting. *J Alzheimers Dis* 44:183–193.

Suppa P, Hampel H, Spies L, Fiebach JB, Dubois B, Buchert R (2015b) Fully Automated Atlas-Based Hippocampus Volumetry for Clinical Routine: Validation in Subjects with Mild Cognitive Impairment from the ADNI Cohort. *J Alzheimers Dis*.

Suthana N a, Krupa A, Donix M, Burggren A, Ekstrom AD, Jones M, Ercoli LM, Miller KJ, Siddarth P, Small GW, Bookheimer SY (2010) Reduced hippocampal CA2, CA3, and dentate gyrus activity in asymptomatic people at genetic risk for Alzheimer's disease. *NeuroImage* 53:1077–1084.

Tamnes CK, Walhovd KB, Engvig A, Grydeland H, Krogsrud SK, Østby Y, Holland D, Dale AM, Fjell AM (2014) Regional hippocampal volumes and development predict learning and memory. *Developmental neuroscience* 36:161–174.

Tang X, Holland D, Dale AM, Younes L, Miller MI (2014) Shape abnormalities of subcortical and ventricular structures in mild cognitive impairment and Alzheimer's disease: detecting, quantifying, and predicting. *Human brain mapping* 35:3701–3725.

Teicher MH, Anderson CM, Polcari A (2012) Childhood maltreatment is associated with reduced volume in the hippocampal subfields CA3, dentate gyrus, and subiculum. *Proceedings of the National Academy of Sciences of the United States of America* 109:E563–E572.

Tepes R, Wang L, Csernansky JG, Neubert P, Heun R, Scheef L, Jessen F (2008) Hippocampal surface analysis in subjective memory impairment, mild cognitive impairment and Alzheimer's dementia. *Dementia and geriatric cognitive disorders* 26:323–329.

Thambisetty M, Wan J, Carass A, An Y, Prince JL, Resnick SM (2010) Longitudinal changes in cortical thickness associated with normal aging. *NeuroImage* 52:1215–1223.

Thomann PA, Wüstenberg T, Nolte HM, Menzel PB, Wolf RC, Essig M, Schröder J (2013) Hippocampal and entorhinal cortex volume decline in cognitively intact elderly. *Psychiatry research* 211:31–36.

Thompson PM, Hayashi KM, De Zubicaray GI, Janke AL, Rose SE, Semple J, Hong MS, Herman DH, Gravano D, Doddrell DM, Toga AW (2004) Mapping hippocampal and ventricular change in Alzheimer disease. *NeuroImage* 22:1754–1766.

Tondelli M, Wilcock GK, Nichelli P, De Jager C a, Jenkinson M, Zamboni G (2012) Structural MRI changes detectable up to ten years before clinical Alzheimer's disease. *Neurobiology of aging* 33:e25–e36.

Treadway MT, Waskom ML, Dillon DG, Holmes AJ, Park MTM, Chakravarty MM, Dutra SJ, Polli FE, Iosifescu D V, Fava M, Gabrieli JDE, Pizzagalli D a (2015) Illness progression, recent stress, and morphometry of hippocampal subfields and medial prefrontal cortex in major depression. *Biological psychiatry* 77:285–294.

Tulving E, Markowitsch HJ (1998) Episodic and declarative memory: role of the hippocampus. *Hippocampus* 8:198–204.

Van Leemput K, Bakkour A, Benner T, Wiggins G, Wald LL, Augustinack J, Dickerson BC, Golland P, Fischl B (2009) Automated segmentation of hippocampal subfields from ultra-high resolution in vivo MRI. *Hippocampus* 19:549–557.

von Gunten A, Kövari E, Bussièrè T, Rivara C-B, Gold G, Bouras C, Hof PR, Giannakopoulos P (2006) Cognitive impact of neuronal pathology in the entorhinal cortex and CA1 field in Alzheimer's disease. *Neurobiology of aging* 27:270–277.

Walhovd KB, Westlye LT, Amlien I, Espeseth T, Reinvang I, Raz N, Agartz I, Salat DH, Greve DN, Fischl B, Dale AM, Fjell AM (2011) Consistent neuroanatomical age-related volume differences across multiple samples. *Neurobiology of aging* 32:916–932.

Wang L, Miller JP, Gado MH, McKeel DW, Rothermich M, Miller MI, Morris JC, Csernansky JG (2006) Abnormalities of hippocampal surface structure in very mild dementia of the Alzheimer type. *NeuroImage* 30:52–60.

Wang L, Swank JS, Glick IE, Gado MH, Miller MI, Morris JC, Csernansky JG (2003) Changes in hippocampal volume and shape across time distinguish dementia of the Alzheimer type from healthy aging. *NeuroImage* 20:667–682.

West MJ, Coleman PD, Flood DG, Troncoso JC (1994) Differences in the pattern of hippocampal neuronal loss in normal ageing and Alzheimer's disease. *Lancet* 344:769–772.

West MJ, Kawas CH, Stewart WF, Rudow GL, Troncoso JC (2004) Hippocampal neurons in pre-clinical Alzheimer's disease. *Neurobiology of aging* 25:1205–1212.

Winterburn JL, Pruessner JC, Chavez S, Schira MM, Lobaugh NJ, Voineskos AN, Chakravarty MM (2013) A novel in vivo atlas of human hippocampal subfields using high-resolution 3 T magnetic resonance imaging. *NeuroImage* 74:254–265.

Wirth M, Villeneuve S, Haase CM, Madison CM, Oh H, Landau SM, Rabinovici GD, Jagust WJ (2013) Associations between Alzheimer disease biomarkers, neurodegeneration, and cognition in cognitively normal older people. *JAMA neurology* 70:1512–1519.

Wisse LEM, Biessels GJ, Geerlings MI (2014a) A Critical Appraisal of the Hippocampal Subfield Segmentation Package in FreeSurfer. *Frontiers in aging neuroscience* 6:261.

Wisse LEM, Biessels GJ, Heringa SM, Kuijf HJ, Koek D (H. . L, Luijten PR, Geerlings MI (2014b) Hippocampal subfield volumes at 7T in early Alzheimer's disease and normal aging. *Neurobiology of aging* 35:2039–2045.

Wisse LEM, Biessels GJ, Stegenga BT, Kooistra M, van der Veen PH, Zwanenburg JJM, van der Graaf Y, Geerlings MI (2015a) Major depressive episodes over the course of 7 years and hippocampal subfield volumes at 7 T MRI: The PREDICT-MR study. *Journal of Affective Disorders* 175 :1-7.

Wisse LEM, Gerritsen L, Zwanenburg JJM, Kuijf HJ, Luijten PR, Biessels GJ, Geerlings MI (2012) Subfields of the hippocampal formation at 7 T MRI: in vivo volumetric assessment. *NeuroImage* 61:1043–1049.

Wisse LEM, Reijmer YD, Telgte A ter, Kuijf HJ, Leemans A, Luijten PR, Koek HL, Geerlings MI, Biessels GJ, Utrecht Vascular Cognitive Impairment (VCI) Study Group (2015b) Hippocampal disconnection in early Alzheimer's disease: a 7 tesla MRI study. *J Alzheimers Dis* 45:1247–1256.

Wolf D, Fischer FU, de Flores R, Chételat G, Fellgiebel A (2015) Differential associations of age with volume and microstructure of hippocampal subfields in healthy older adults. *Hum Brain Mapp*.

Yang X, Goh A, Chen S-HA, Qiu A (2013) Evolution of hippocampal shapes across the human lifespan. *Human brain mapping* 34:3075–3085.

Yassa M a, Muftuler LT, Stark CEL (2010a) Ultrahigh-resolution microstructural diffusion tensor imaging reveals perforant path degradation in aged humans in vivo. *Proceedings of the National Academy of Sciences of the United States of America* 107:12687–12691.

Yassa M a, Stark CEL (2011) Pattern separation in the hippocampus. *Trends in neurosciences* 34:515–525.

Yassa M a, Stark SM, Bakker A, Albert MS, Gallagher M, Stark CEL (2010b) High-resolution structural and functional MRI of hippocampal CA3 and dentate gyrus in patients with amnesic Mild Cognitive Impairment. *NeuroImage* 51:1242–1252.

Ye BS et al. (2014) Hippocampal and cortical atrophy in amyloid-negative mild cognitive impairments: comparison with amyloid-positive mild cognitive impairment. *Neurobiology of aging* 35:291–300.

Yushkevich PA et al. (2015a) Quantitative comparison of 21 protocols for labeling hippocampal subfields and parahippocampal subregions in in vivo MRI: towards a harmonized segmentation protocol. *Neuroimage* 111:526–541.

Yushkevich PA, Pluta JB, Wang H, Xie L, Ding S-L, Gertje EC, Mancuso L, Kliot D, Das SR, Wolk D a (2015b) Automated volumetry and regional thickness analysis of hippocampal subfields and medial temporal cortical structures in mild cognitive impairment. *Human brain mapping* 36:258–287.

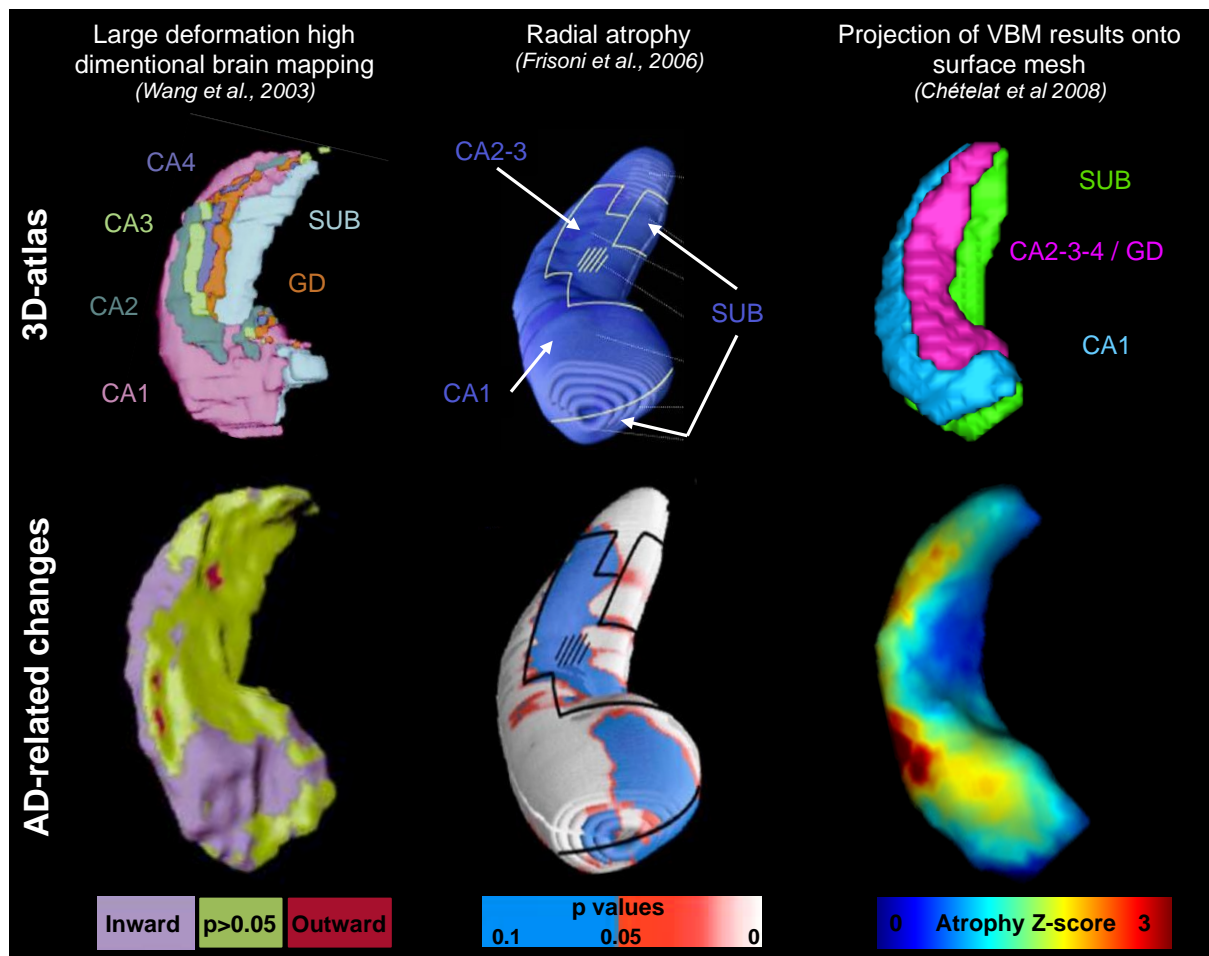
Yushkevich PA, Wang H, Pluta J, Das SR, Craige C, Avants BB, Weiner MW, Mueller S (2010) Nearly automatic segmentation of hippocampal subfields in in vivo focal T2-weighted MRI. *NeuroImage* 53:1208–1224.

Zeineh MM, Holdsworth S, Skare S, Atlas SW, Bammer R (2012) Ultra-high resolution diffusion tensor imaging of the microscopic pathways of the medial temporal lobe. *NeuroImage* 62:2065–2082.

Ziegler G, Dahnke R, Jäncke L, Yotter RA, May A, Gaser C (2011) Brain structural trajectories over the adult lifespan. *Human brain mapping* 33:2377–2389.

Figures.

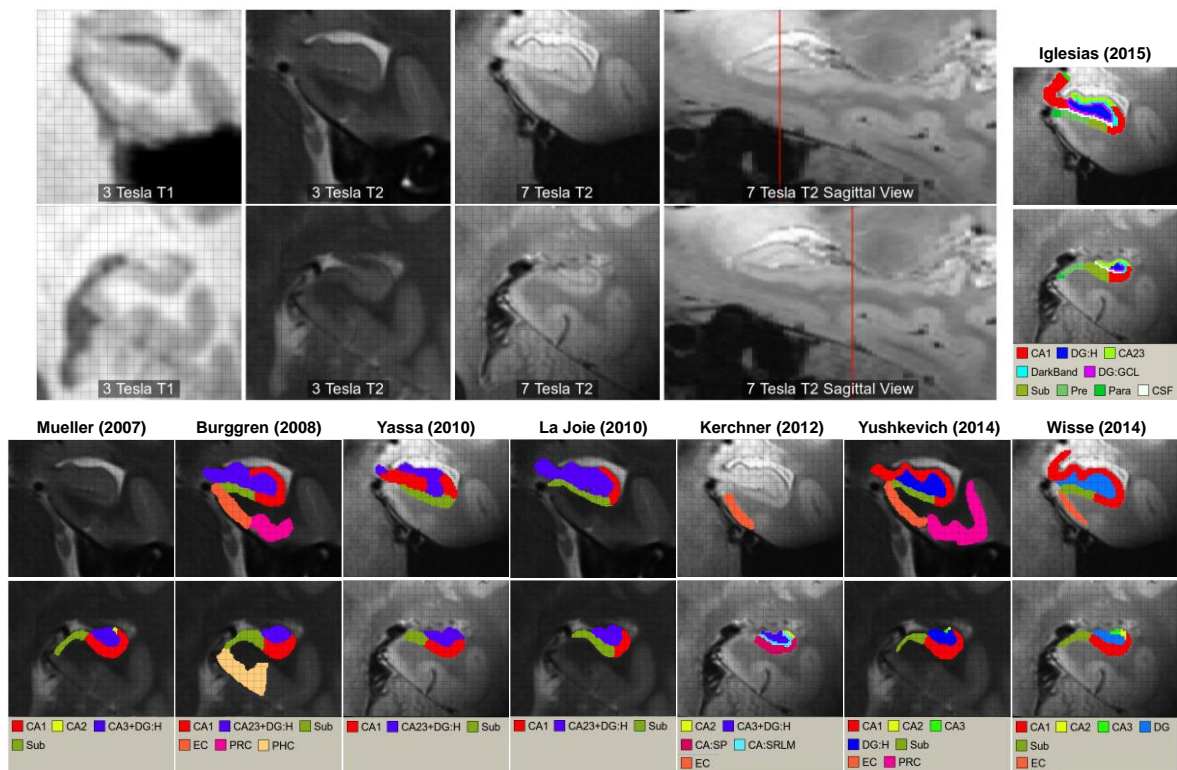
Figure 1. Surface-based methods to assess hippocampal subfield atrophy in AD.



The figure illustrates the pattern of hippocampal subfield atrophy in AD (as compared to healthy controls) evidenced using three different methods. For the sake of simplicity, only the right hippocampus is presented (from a superior view). Top row shows the atlas used by each group to determine the localization of subfield on the hippocampal surface while bottom row shows the pattern of atrophy in AD. All three methods show a strong atrophy along the lateral zone of the hippocampus, corresponding to the CA1 subfield.

Figures are reproduced from: (left column) Wang et al., Neuroimage 2003, with permission from Elsevier ; (middle column) Frisoni et al., Neuroimage (2006), with permission from Elsevier ; (right column) Chételat et al., Neuropsychologia (2008), with permission from Elsevier.

Figure 2. Subfield segmentation : variations in image acquisition and segmentation protocols.



The figure shows the left hippocampus of a 36 yo healthy control acquired with different scanners (1.5T, 3T, 7T) and segmented by multiple groups (using their own segmentation protocol/atlas) participating in the Hippocampal Subfields Group. The top slice corresponds to the head while the bottom slice shows the body of the hippocampus. The lower panel of each segmentation example indicates which substructures were segmented in each protocol.

Figure is reproduced from: Yushkevich et al., Neuroimage 2015, with permission from Elsevier.

Table 1: Overview of studies investigating hippocampal subfield structural changes over the course of AD

Study	Field strength (T), Weighting, Resolution before interpolation (mm3)	Segmentation	Population number (mean age \pm SD) / range	Labeled subfields	Subfields affected
Adachi et al., (2003)	1.5 T, T2, 1.0 x 1.0 x 1.0	Manual	mild AD : n = 12 (67.9 \pm 7.1) moderate AD : n = 14 (70.0 \pm 7.8)	Sub, CA1, CA3/4	mild AD: CA1 and sub moderate AD: CA1, sub and CA3/4
Mueller et al. (2010)	4 T, T2, 0.4 x 0.4 x 2.1	Manual	MCI : n = 20 (73.6 \pm 7.1) AD : n = 18 (69.1 \pm 9.5)	Sub, CA1, CA1-2 transition, CA3/DG	MCI : CA1-2 transition AD : sub, CA1, CA1-2 transition
Mueller and Weiner (2009)*	4 T, T2, 0.4 x 0.4 x 2.0	Manual	MCI : n = 20 (73.5 \pm 7.1) AD : n = 18 (69.1 \pm 9.6)	Sub, CA1, CA1-2 transition, CA3/DG	MCI : CA1-2 transition AD : sub, CA1, CA1-2 transition
Kerchner et al., (2010)	7 T, T2*, 0.195 x 0.195 x 2.0	Manual	mild AD : n = 14 (66 \pm 8)	CA1-SRLM, CA1-SP	CA1-SRLM
Yassa et al. (2010)	3 T, T1, 0.75 x 0.75 x 0.75	Manual	MCI : n = 10 (76 \pm 7)	Sub, CA1, CA3/DG	CA1 and CA3/DG
Kerchner et al. (2013)	7 T, T2, 0.22 x 0.22 x 1.5	Semi-automated	MCI : n = 15 (73.2 \pm 5.5) mild AD : n = 11 (69.5 \pm 9.3)	CA1-SRLM, CA1-SP, CA3/DG	MCI : no effect mild AD : CA1-SRLM, CA1-SP, CA3/DG
Pluta et al. (2012)	3 T, T2, 0.4 x 0.4 x 2.0	Semi-automated (ASHS)	MCI : n = 17 (70.2 \pm 7.6)	CA1, CA4/DG	CA1, CA4/DG
de Flores et al. (2015)	3 T, PD, 0.375 x 0.375 x 2.0	Manual	MCI : n = 17 (71.7 \pm 6) AD : n = 18 (67.4 \pm 9.9)	Sub, CA1, CA2/3/4/DG	MCI : CA1, sub AD : CA1, sub, CA2/3/4/DG
La Joie et al., (2013)*	3 T, PD, 0.375 x 0.375 x 2.0	Manual	MCI : n = 17 (71.7 \pm 6) AD : n = 18 (67.4 \pm 9.9)	Sub, CA1, CA2/3/4/DG	MCI : CA1, sub AD : CA1, sub, CA2/3/4/DG
Wisse et al. (2014b)	3 T, T2, 0.7 x 0.7 x 0.7	Manual	MCI : n = 16 (74.4 \pm 9) AD : n = 9 (70.8 \pm 8.4)	Sub, CA1, CA2, CA3, CA4/DG	MCI : no effect AD : sub, CA1, CA3, CA4/DG
Boutet et al. (2014)	7 T, T2*, 0.3 x 0.3 x 1.2	Manual	AD: n = 4 (65.8 \pm 7.0)	CA1-SRLM, CA1-SP, hilum, sub-SP, alveus	CA1-SRLM, CA1-SP, sub-SP, alveus
Yushkevich et al. (2015b)	3 T, T2, 0.4 x 0.4 x 2.0	Automated (ASHS)	MCI : n = 40 (71.8 \pm 7.0)	Sub, CA1, CA2, CA3, DG	CA1, CA2, DG

Csernansky et al. (2000)	1.5 T, T1, 1.0 x 1.0 x 1.0	LD HDBM	early DAT : n = 18 (74.0 ± 4.8)	Sub, CA1, CA2/3/4/DG	CA1
Wang et al. (2006)	1.5 T, T1, 1.0 x 1.0 x 1.0	LD HDBM	mild AD : n = 49 (74.9 ± 7.8)	Sub, CA1, CA2/3/4/DG	CA1, sub
Wang et al. (2003)*	1.5 T, T1, 1.0 x 1.0 x 1.0	LD HDBM	mild AD : n = 18 (74 ± 4.4)	Sub, CA1, CA2/3/4/DG	CA1, sub
Frisoni et al. (2006)	1 T, T1, 1.3 x 1.3 x 1.3	Radial Atrophy mapping	AD : n= 28 (73.8 ± 9.4)	Presub, sub, CA1, CA2/3, fimbria	CA1, sub
Frisoni et al. (2008)	3 T, T1, 1.0 x 1.0 x 1.0	Radial Atrophy mapping	AD : n = 19 (76.1 ± 5.7)	Presub, sub, CA1, CA2/3, fimbria	presub, sub, CA1
Chételat et al. (2008)	1.5 T, T1, 1.0 x 1.0 x 1.5	VBM (surface mapping)	MCI : n = 17 (71.4 ± 8.6) AD : n = 17 (69.4 ± 5.4)	Sub, CA1, CA2/3/4/DG	MCI : CA1 AD : CA1, CA2/3/4/DG
Tepest et al. (2008)	1.5 T, T1, 1.0 x 1.0 x 1.0	LD HDBM	MCI : n = 15 (68.2 ± 5.4) AD : n = 12 (69.2 ± 10.0)	Sub, CA1, CA2/3/4/DG	MCI : CA1 AD : CA1
Gerardin et al. (2009)	1.5 T, T1, 0.9375 x 0.9375 x 1.5	Spherical harmonics	MCI : n = 23 (74 ± 8) AD : n = 23 (73 ± 6)		MCI : CA1 AD : CA1
Piaveni et al. (2011)	1 T, T1, 1.3 x 1.3 x 1.3	Radial Atrophy mapping	AD APOE4 carriers: n = 14 (71.2 ± 9.5) AD APOE4 non carriers: n = 14 (71.7 ± 8.2)	Presub, sub, CA1, CA2/3, fimbria	AD APOE4 carriers: sub, CA1 AD APOE4 non-carriers: sub, CA1
Atienza et al. (2011)	1.5 T, T1, 1.2 x 1.2 x 1.2	VBM (maps :Amunts et al., 2005)	MCI : n = 32 (69.1 ± 6.1)	Sub, CA,DG	Sub, CA,DG
Chow et al. (2012)	Subjects were scanned at five different sites	Radial Atrophy mapping	AD : n = 55 (74.8 ± 7.4)	Sub, CA1, CA2/3	all subfields
Apostolova et al. (2012)	1.5 T, T1, 0.9 x 0.9 x 1.5	Radial Atrophy mapping	MCI : n = 33 (73.1 ± 6.0) AD : n = 43 (75.7 ± 7.6)	Sub, CA1, CA2/3	MCI : sub, CA2/3 AD : all subfields
Tang et al. (2014)	ADNI	Vertex-Based Statistical Analysis	MCI : n = 369 (75 ± 7.3) AD : n = 175 (75.3 ± 7.5)	Sub, CA1, CA2/3/DG	MCI : CA1 AD : CA1
Chow et al. (2015)	1.5 T, T1, 1.25 x 1.25 x 1.2	Radial Atrophy mapping	MCI : n = 76 (75.2 ± 8.2) AD : n = 37 (74.1 ± 8.7)	Sub, CA1, CA2/3	MCI : sub, CA1, CA2 AD : sub, CA1, CA2
	3 T, T1, 1 x 1 x 1.2				

Hanseeuw et al. (2011)	3 T, T1, 0.81 x 0.95 x 1.0	FreeSurfer 5	MCI : n= 15 (72.3 ± 7.3)	Presub, sub, CA1, CA2/3, CA4/DG, Fimbria	sub, CA2/3
Lim et al. (2012)	3 T, T1, 1.0 x 1.0 x 1.0	FreeSurfer 5	MCI : n= 45 (73.7 ± 6.4)	Presub, sub, CA1, CA2/3, CA4/DG, Fimbria	Presub, sub, CA2/3
Lim et al. (2013)	3 T, T1, 1.0 x 1.0 x 1.0	FreeSurfer 5	AD : n = 31 (75.0 ± 8.5)	Presub, sub, CA1, CA2/3, CA4/DG, Fimbria	Presub, sub, CA2/4, CA4/DG
Li et al. (2013)	1.5 T, T1, 1.2 x 1.2 x 1.2	FreeSurfer 5	mild AD : n = 29 (73.1 ± 7.4)	Presub, sub, CA1, CA2/3, CA4/DG, Fimbria	Presub, sub, CA1, CA2/3, CA4/DG, Fimbria
Khan et al., (2014)	1.5 T, T1, 1.1 x 1.1 x 1.2	FreeSurfer 5	Stable MCI : n= 357 (75.1 ± 7.0) MCI converters: n = 90 (74.1 ± 6.6) AD: n = 291 (75.4 ± 7.0)	Presub, sub, CA1, CA2/3, CA4/DG, Fimbria	Stable MCI : Presub, sub, CA1, CA2/3, CA4/DG, Fimbria MCI converters: Presub, sub, CA1, CA2/3, CA4/DG, Fimbria AD: Presub, sub, CA1, CA2/3, CA4/DG, Fimbria
Yushkevich et al. (2015b)	3 T, T1, 1.0 x 1.0 x 1.0	FreeSurfer 5	MCI : n = 40 (71.8 ± 7.0)	Presub, sub, CA1, CA2/3, CA4/DG, Fimbria	Presub, sub, CA2/3, CA4/DG, Fimbria
Iglesias et al. (2015)	ADNI, T1, 1.0 x 1.0 x 1.0 T2, 0.4 x 0.4 x 2	FreeSurfer 6	MCI : n = 16 (74.3 ± 7.6)	Alveus, parasub, presub, sub, CA1, CA2/3, CA4, GC-DG, Fimbria, molecular layer	CA1, CA2/3, CA4, GC-DG, Fimbria, molecular layer

*: Study performed on a partly overlapping sample with the study presented above

PD: Proton Density, LD HDBM: Large-Deformation High-Dimensional Brain Mapping, ASHS: Automatic Segmentation of Hippocampal Subfields, VBM: Voxel Based Morphometry, sub: subiculum, presub: presubiculum, parasub: parasubiculum, GC-DG: granule cell layer of dentate gyrus CA: Cornu Ammonis, , DG: Dentate Gyrus, SRLM: Stratum Radiatum and Stratum Lacunosum-Moleculare, SP: Stratum Pyramidale; ADNI: Alzheimer's Disease Neuroimaging Initiative.

Note that only the hippocampal subfields are considered in this review including in the Tables, even when other regions (e.g. parahippocampal areas) were investigated

Table 2: Overview of studies investigating hippocampal subfield structural changes in healthy controls carrying the APOE4 allele.

Study	Field strength (T), Weighting, Resolution before interpolation (mm3)	Segmentation	Population number (mean age \pm SD) / range	Labeled subfields	Results
Mueller et al. (2008)	4 T, T2, 0.4 x 0.4 x 2.0	Manual	Young APOE4 non-carriers: n = 19 (46.8 \pm 10.5) Young APOE4 carriers: n = 9 (50.8 \pm 8.1) Old APOE4 non-carriers: n = 24 (71.29 \pm 7.6) Old APOE4 carriers: n = 14 (69.2 \pm 6.0)	Sub, CA1, CA1-2 transition, CA3/DG	Effect on CA3/DG
Mueller & Weiner (2009)*	4 T, T2, 0.4 x 0.4 x 2.0	Manual	n = 66 (61.0 \pm 13.9) APOE4 non-carriers: n = 43 APOE4 carriers: n = 23	Sub, CA1, CA1-2 transition, CA3/DG	Effect on CA3/DG
Donix et al. (2010a)	3 T, T2, 0.39 x 0.39 x 3.0	Manual	Family history of AD: n = 26 (63.5 \pm 9.8) APOE4 non-carriers n = 13 APOE4 carriers: n = 13 No family history of AD: n = 25 (61.0 \pm 11.6) APOE4 non-carriers: n = 13 APOE4 carriers: n = 12	Sub, CA1, CA2/3/DG	Effect on sub thickness (for both APOE4 and family history)
Burggren et al. (2008)*	3 T, T2, 0.39 x 0.39 x 3.0	Manual	APOE4 non-carriers: n = 16 (57.3 \pm 7.8) APOE4 carriers: n = 14 (57.7 \pm 9.6)	Sub, CA1, CA2/3/DG	Effect on sub thickness
Donix et al. (2010b)* <i>Longitudinal study</i>	3 T, T2, 0.39 x 0.39 x 3.0	Manual	APOE4 non-carriers: n = 16 (60.1 \pm 7.1) APOE4 carriers: n = 16 (61.7 \pm 11.5)	Sub, CA1, CA2/3/DG	Effect on sub thickness

*: Study performed on a partly overlapping sample with the study presented above

sub: subiculum, presub: presubiculum, CA: Cornu Ammonis, DG: Dentate Gyrus, SRLM: Stratum Radiatum and Stratum Lacunosum-Moleculare, SP: Stratum Pyramidale

Note that only the hippocampal subfields are considered in this review including in the Tables, even when other regions (e.g. parahippocampal areas) were investigated.

Table 3: Overview of studies investigating hippocampal subfields structural change over the course of normal aging

Study	Field strength (T), Weighting, Resolution before interpolation (mm3)	Segmentation	Population number (mean age \pm SD) / range	Labeled subfields	Results
Mueller et Weiner (2009)	4 T, T2, 0.4 x 0.4 x 2.0	Manual	n = 119 (53.4 \pm 17.2) / 22-85 years	Sub, CA1, CA1-2 transition, CA3/DG	Linear diminution of CA1 and CA3/DG
Mueller et al. (2007)*	4 T, T2, 0.4 x 0.5 x 2.0	Manual	n = 42 (48.7) / 21-85 years	Sub, CA1, CA2, CA3/4/DG	Linear diminution of CA1
de Flores et al. 2015	3 T, PD, 0.375 x 0.375 x 2.0	Manual	n = 98 (45.7 \pm 19.2)	Sub, CA1, CA2/3/4/DG	Linear diminution of sub Non-linear diminution of CA1
La Joie et al. (2010)*	3 T, PD, 0.375 x 0.375 x 2.0	Manual	n = 50 (39.9 \pm 15.2) / 19 -68 years	Sub, CA1, CA2/3/4/DG	Linear diminution of sub
Shing et al. (2011)	3 T, PD, 0.4 x 0.4 x 2.1	Manual	older: n = 19 (75.4 \pm 2.9) / 70-78 years younger : n= 10 (23 \pm 1.7) / 20-25 years	Sub, CA1/2, CA3/4/DG	Diminution of CA1/2
Kerchner et al. (2013)	7 T, T2, 0.22 x 0.22 x 1.5	Manual / semi-automated	older : n = 18 (70.2 \pm 6.2) younger : n= 9 (28.2 \pm 4.1)	CA1-SRLM, CA1-SP, CA3/DG	Diminution of CA1-SRLM
Wisse et al. (2014b)	7 T, T2, 0.7 x 0.7 x 0.7	Manual	n = 29 (70.2 \pm 3.5)	Sub, CA1, CA2, CA3, CA4/DG	Linear diminution of CA1 and DG/CA4
Raz et al. (2014)	3 T, PD, 0.4 x 0.4 x 2.0	Manual	n = 80 (57.84 \pm 14.27) / 22-82 years	Sub, CA1/2, CA3/DG	Linear diminution of CA1/2
Csernansky et al. (2000)	1.5 T, T1, 1.0 x 1.0 x 1.0	LD HDBM	older : n = 18 (74.2 \pm 5.2) younger : n= 15 (30.9 \pm 9.0)	Sub, CA1, CA2/3/4/DG	Diminution of the head and tail
Wang et al. (2006)	1.5 T, T1, 1.0 x 1.0 x 1.0	LD HDBM	n = 86 (73.4 \pm 11) / 50 - 91 years	Sub, CA1, CA2/3/4/DG	Linear diminution of all subfields
Wang et al. (2003)*	1.5 T, T1, 1.0 x 1.0 x 1.0	LD HDBM	n = 26 (73 \pm 7)	Sub, CA1, CA2/3/4/DG	Diminution of sub
Chételat et al. (2008)	1.5 T, T1, 1.0 x 1.0 x 1.5	VBM (surface mapping)	n = 59 (48.4 \pm 18) / 20-84 years	Sub, CA1, CA2/3/4/DG	Linear diminution of sub

Frisoni et al. (2008)	3 T, T1, 1.0 x 1.0 x 1.0	Radial atrophy mapping	n = 19 (73.6 ± 5.5) / 66-82 years	Presub, sub, CA1, fimbria	diminution of CA1 and presub
Ziegler et al. (2011)	1.5 / 3 T, T1, 0.93 x 0.93 x 1.2	VBM (maps :Amunts et al., 2005)	n = 547 (48.1 ± 16.6) / 19-86 years	Sub, CA, DG	Linear diminution of sub Non-linear diminution of CA, DG
Apostolova et al. (2012)	1.5 T, T1, 0.9 x 0.9 x 1.5	Radial distance mapping	n = 46 (66.4 ± 7.8)	Sub, CA1, CA2/3	diminution of all subfields
Thomann et al. (2013)	1.5 T, T1, 0.98 x 0.98 x 1.8	VBM (maps :Amunts et al., 2005) Shape analysis (FSL-FIRST)	older : n = 20 (74.15 ± 0.75) / 73-75 years younger : n= 20 (54.40 ± 0.68) / 53-55 years	VBM: sub, CA, DG Shape analysis: sub, CA1, CA2/3/4/DG	diminution of sub, CA
Yang et al. (2013)	1.5 T, T1, 1.0 x 1.0 x 1.25	LD HDBM	n = 302 (44.5 ± 23.8) / 18 - 94 years	Sub, CA1, CA2/3/4/DG	Effects on head and sub
Pereira et al. (2014)	3 T, T1, 1.0 x 1.0 x 1.0	FreeSurfer 5	n = 50 (63.7 ± 7.0) / 50-75 years	Presub, sub, CA1, CA2/3, CA4/DG, Fimbria	Linear diminution of CA2/3 and CA4/DG

*: Study performed on a partly overlapping sample with the study presented above

PD: Proton Density, LD HDBM: Large-Deformation High-Dimensional Brain Mapping, ASHS: Automatic Segmentation of Hippocampal Subfields, VBM: Voxel Based Morphometry, sub: subiculum, presub: presubiculum,

CA: Cornu Ammonis, DG: Dentate Gyrus, SRLM: Stratum Radiatum and Stratum Lacunosum-Moleculare, SP: Stratum Pyramidale

Note that only the hippocampal subfields are considered in this review including in the Tables, even when other regions (e.g. parahippocampal areas) were investigated.